



**HAL**  
open science

## Ambipolar discotic liquid crystals built around platinum diimine-dithiolene cores

Franck Camerel, Corinne Lagrost, Marc Fourmigué, Grégory Albert, Frédéric Barrière, Olivier Jeannin

► **To cite this version:**

Franck Camerel, Corinne Lagrost, Marc Fourmigué, Grégory Albert, Frédéric Barrière, et al.. Ambipolar discotic liquid crystals built around platinum diimine-dithiolene cores. *Chemistry - A European Journal*, 2019, 25 (22), pp.5719-5732. 10.1002/chem.201806304 . hal-02015935

**HAL Id: hal-02015935**

**<https://univ-rennes.hal.science/hal-02015935>**

Submitted on 28 Feb 2019

**HAL** is a multi-disciplinary open access archive for the deposit and dissemination of scientific research documents, whether they are published or not. The documents may come from teaching and research institutions in France or abroad, or from public or private research centers.

L'archive ouverte pluridisciplinaire **HAL**, est destinée au dépôt et à la diffusion de documents scientifiques de niveau recherche, publiés ou non, émanant des établissements d'enseignement et de recherche français ou étrangers, des laboratoires publics ou privés.

# Ambipolar discotic liquid crystals built around platinum diimine-dithiolene cores

Franck Camerel,<sup>1,\*</sup> Grégory Albert,<sup>1</sup> Frédéric Barrière,<sup>1</sup> Corinne Lagrost,<sup>1</sup> Marc Fourmigué,<sup>1</sup> Olivier Jeannin<sup>1</sup>

1) Univ Rennes, CNRS, ISCR - UMR 6226, F-35000 Rennes, France. Email :  
franck.camerel@univ-rennes1.fr

## Abstract

Platinum diimine dithiolene complexes bearing mesogenic groups on one or both ligands have been prepared through an original ligand metathesis reaction to introduce the dithiolene ligand. The neutral diimine ligands, the intermediate platinum dichloride diimine complexes and the target compounds were characterized by a combination of electronic (electrochemistry, absorption and emission spectroscopy, DFT calculations) and structural (SAXS, DSC) tools. Several novel liquid crystalline platinum diimine-dithiolene were identified over a large temperature range, furthermore endowed with ambipolar properties, associated with the high reversibility of both oxidation and reduction processes.

## Introduction

Discotic Liquid Crystals (DLSs) have attracted a lot of interest due to their charge transport properties, their ability to be easily aligned in thin films and their self-healing capability for applications in optoelectronic as active layers in OLED, OFET and solar cells.<sup>[1]</sup> Ambipolar DLCs are particularly appealing since they are able to simultaneously carry electrons and holes and new designs are developed to obtain novel ambipolar semiconducting soft materials.<sup>[2]</sup>

Most examples of DLC semiconductors with ambipolar properties are purely organic compounds, such as triphenylenes or phthalocyanines,<sup>[3]</sup> while ambipolar charge transport has also been reported in triazine-based columnar liquid crystals.<sup>[4]</sup> In the latter, the triazine discotic core acts as an electron accepting unit whereas the peripheral thiophene units provide electron-donating properties. Another organic ambipolar DLC was obtained by covalently grafting a phthalocyanine as an electron-donor and a fullerene as an electron acceptor.<sup>[5]</sup> Muller and co-workers also reported an ambipolar DLC with n-type perylene monoimide (PMI) covalently linked around p-type hexabenzocoronene core.<sup>[6]</sup> Large ambipolar carrier mobility was also found in discotic liquid crystalline truxenes substituted with alkyl chains at bay-positions.<sup>[7]</sup> More recently, a DLC material, consisting of a planarized triphenylborane mesogen, was reported to form a hexagonal columnar LC phase exhibiting ambipolar carrier transport properties with electron and hole mobility.<sup>[8]</sup>

Besides, the number of ambipolar DLC built around metal complexes remains scarce. The only examples involve gadolinium or zinc phthalocyanines<sup>[9,10]</sup> and very recently, ambipolar carrier mobility was mentioned for a series of liquid crystalline platinum (II) complexes with 2-phenylpyridine derivatives as the main ligand and 5-substituted tetrazole as the auxiliary ligand.<sup>[11]</sup>

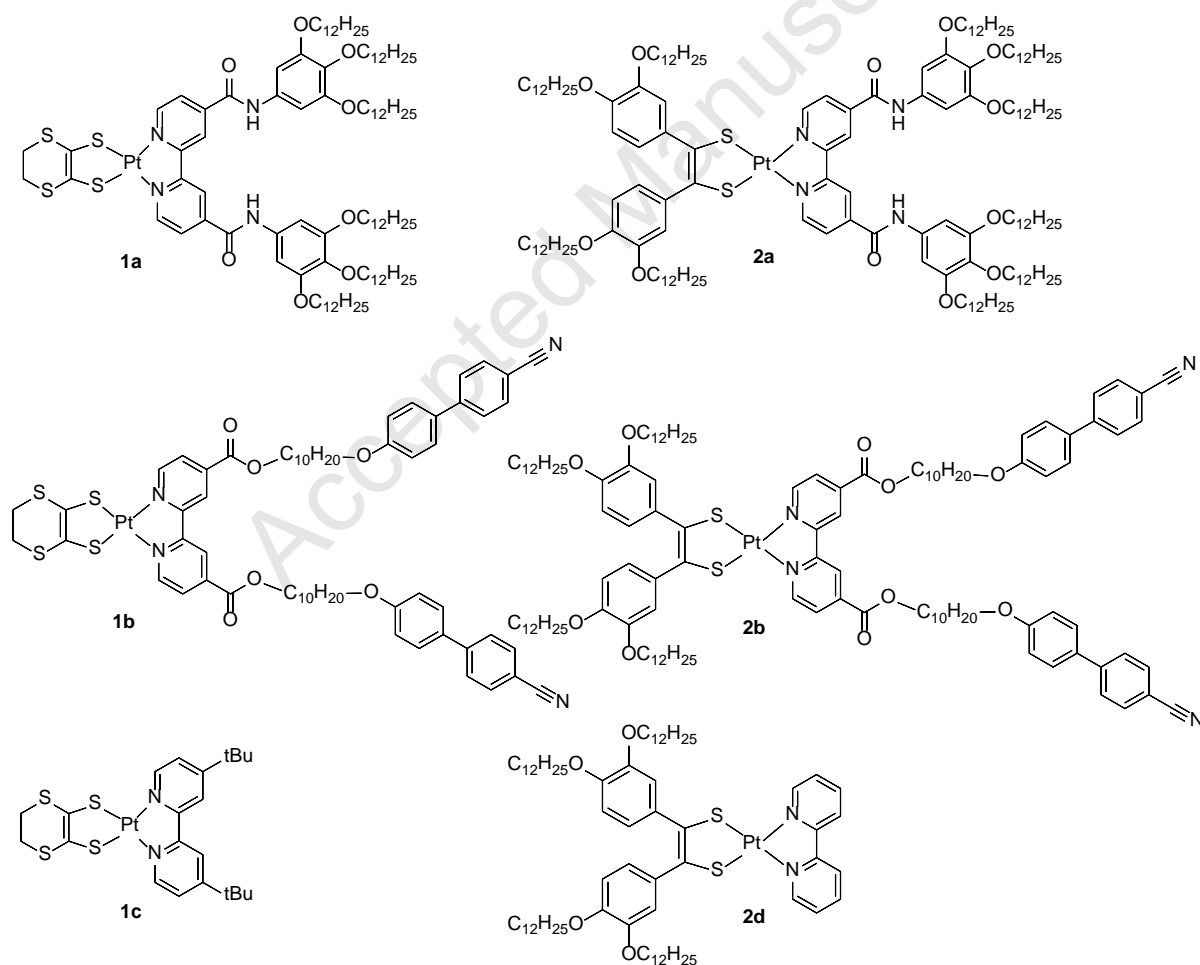
In that respect, neutral platinum diimine-dithiolene complexes formulated as  $[\text{Pt}^{\text{II}}(\text{diimine})(\text{dithiolato})]^{0}$  are an interesting class of ambipolar complexes with heteroleptic ligands. Indeed, the diimine fragment is prone to undergo reduction at relatively accessible potentials whereas the electron-rich dithiolene fragment is easily oxidized. Several research groups<sup>[12]</sup> and in particular the group of R. Eisenberg<sup>[13]</sup> have developed the synthesis of platinum diimine-dithiolene complexes to understand and to modulate their photophysical and redox properties. Complexes have been prepared by using 2,2'-bipyridine or 1,10-phenanthroline as diimine ligands and 1,2-benzenedithiolates, 1,1-dithiolates or 1,2-

ethylenedithiolates as dithiolate ligands. These square planar  $[\text{Pt}^{\text{II}}(\text{diimine})(\text{dithiolato})]^0$  complexes also display solution luminescence and solvatochromic absorption bands which are attributed to common charge-transfer bands. Diimine-dithiolene complexes have also been proposed as light harvester in the visible region for light driven aqueous reduction to hydrogen<sup>[14]</sup> but also in solar cells.<sup>[15]</sup> Crown ethers have been introduced on the dithiolate ligand in the  $[\text{Pt}(\text{NN})(\text{SS})]$  system for developing optical and electrochemical sensors for alkali metal cations.<sup>[16]</sup>

Surprisingly and to the best of our knowledge, only one liquid crystalline material build around a metal diimine-dithiolene core has been described up to now by Ho-Chol Chang and coworkers in 2011.<sup>[17]</sup> A platinum complex having an asymmetric molecular structure derived from 1,2-benzenedithiolato (bdt) and a bipyridine ligand carrying ramified C8 or C10 carbon chains forms a columnar mesophase of hexagonal symmetry over a large temperature range from  $-18\text{ }^\circ\text{C}$  up to  $194\text{ }^\circ\text{C}$ . This complex undergoes quasi reversible one-electron reduction at  $-1.89\text{ V}$  vs  $\text{Fc}/\text{Fc}^+$  that corresponds to bpy-based reduction processes. The dithiolate ligand can also be oxidized but according to a slow electrochemical process because the peak-to-peak separation of this oxidation process is found to be  $0.17\text{ V}$ , far above the expected value for a nernstian one-electron transfer process ( $0.059\text{ V}$ ).

Thus, to obtain new ambipolar discotic liquid crystals, four diimine-dithiolene complexes, differently functionalized by long carbon chains or cyanobiphenyl fragments, have been developed herein by using a ligand metathesis between dichloroplatinum diimine derivatives and tin or nickel dithiolene complexes as dithiolate ligand precursors (Scheme 1). The platinum complexes carry a 5,6-dihydro-1,4-dithiin-2,3-dithiolato (dddtd) ligand (in **1a-c**) or a 1,2-bis(3,4-bis(dodecyloxy)phenyl)ethene-1,2-bis(thiolato) ( $\text{C}_{12}\text{dt}$ ) ligand (in **2a**, **2b** and **2d**) and as diimine ligand, a functional bipyridine carrying, either tris-dodecyloxyphenyl fragments connected through an amide linker and noted  $\text{bpyC}_{12}$  (in **1a** and **2a**) or cyanobiphenyl

fragments connected through an ester linker carrying a C10 carbon chains and noted bpyCBP (in **1b** and **2b**). Compounds **1c** and **2d** have been synthesized as reference compounds. The electronic properties of these complexes and their precursors have been characterized by absorption and luminescence spectroscopies as well as by cyclic voltammetry and DFT calculations. The structural properties of these compounds were also investigated by a combination of optical microscopy under crossed polarizers, DSC analyses and small angle X-ray diffraction. The results obtained confirmed that these compounds have indeed a strong ambipolar character with good reversibility and that some of them also display liquid crystalline properties over a large temperature range.



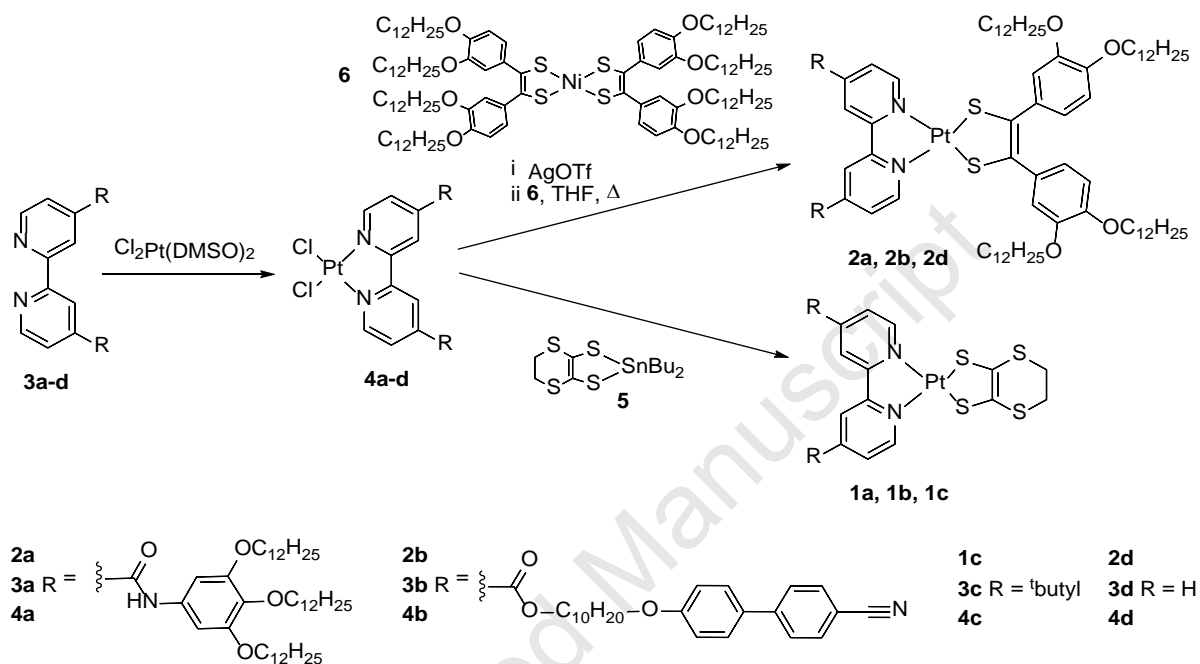
**Scheme 1.** Chemical structure and name of the functional diimine-dithiolenes complexes investigated.

## Results and discussion

### Synthesis and characterization

Synthetic routes toward the functional diimine-dithiolene compounds are presented in Scheme

2. Full synthetic details are given in the experimental part.



**Scheme 2.** Synthetic routes used for the preparation of the functional diimine-dithiolene platinum complexes.

First, functional bipyridine carrying either tris-dodecyloxyphenyl fragments connected through an amide linker (bpyC<sub>12</sub> **3a**), or cyanobiphenyl fragments connected through ester linker carrying a C<sub>10</sub> carbon chains (bpyCBP **3b**) were reacted with 1 eq. of PtCl<sub>2</sub>(DMSO)<sub>2</sub> to afford the corresponding dichloroplatinum diimine complexes **4a** and **4b** in 76 and 52 % yield, respectively. The synthesis of these two functional bipyridine molecules **3a** and **3b** is fully described in the experimental part. For introducing the ddt dithiolene ligand, dichloroplatinum diimine complexes **4a-b** were then reacted with one equivalent of 2,2-dibutyl-5,6-dihydro-1,3,2-dithiastannolo[4,5-b][1,4]dithiin **5** in acetone to afford **1a** (75 % yield) and **1b** (63 %

yield) as green powders. For introducing the C<sub>12</sub>dt dithiolene ligand to prepare in the **2a** and **2b** complexes, the dichloroplatinum diimine complexes **4a-b** were first reacted with silver triflate in order to exchange the chloride ligand by the more labile triflate anion. The triflate derivative was then refluxed with the neutral nickel bis(dithiolene) complex **6** in THF to afford after purification the expected compounds **2a** and **2b**. EDX analyses have also revealed that there is no trace of nickel in the isolated compounds.

The reference compounds **1c** and **2d** were prepared in a similar way. The dddt derivative **1c** was readily obtained from the reaction of the dichloroplatinum diimine complex **4c** with one equivalent of **5** in acetone, while **2d** was also obtained in 28 % yield by first reacting [PtCl<sub>2</sub>(bpy)] **3d** with silver triflate followed by reaction with **6**.

The purity and the molecular structure of all the compounds were confirmed by elemental analyses, <sup>1</sup>H NMR and <sup>13</sup>C NMR spectroscopy, UV-vis, mass spectroscopy and IR spectroscopy. The introduction of Cl<sub>2</sub>Pt on the bipyridine fragments is characterized by a down-field shift of the <sup>1</sup>H signal of bipyridine protons. The introduction of the dddt fragment in place of the two chloride ligands results in a singlet between 2.61 and 3.51 ppm integrating for 4H corresponding to the hydrogen atoms of the S-CH<sub>2</sub> groups. Despite several attempts in CDCl<sub>3</sub>, d<sub>6</sub>-DMSO and CD<sub>2</sub>Cl<sub>2</sub> at room temperature but also at 60 °C, the two complexes **2a** and **2b** bearing long alkyl chains on both the dithiolene and the diimine ligands could not be properly characterized by NMR spectroscopy, likely due to strong aggregation effects in solution (vide infra). However, the optical, thermal and electronic properties as well as the mass spectroscopy and the elemental analysis unambiguously confirmed the formation of the expected complexes.

### **X-ray structure of 1c**

Single-crystals suitable for X-ray diffraction of the model compound **1c** with the dddt and (tBu)<sub>2</sub>bpy ligands were obtained in CHCl<sub>3</sub> by slow diffusion of pentane. Crystallographic data

are given in Table S1-S4. This compound crystallizes as chloroform solvate in the triclinic system, space group  $P\bar{1}$  ( $a = 7.2116(4)$  Å;  $b = 13.8530(9)$  Å;  $c = 15.3854(10)$  Å;  $\alpha = 69.100(2)^\circ$ ;  $\beta = 86.336(2)^\circ$ ;  $\gamma = 82.782(2)^\circ$ ;  $V = 1424.23(15)$  Å<sup>3</sup>,  $Z = 2$ ). Figure 1 shows the atomic numbering scheme and a projection of the crystalline structure along  $a$ . The asymmetric unit contains one complex and one chloroform molecule, both in general position. The X-ray crystal structure confirms the chemical structure of the complex. The platinum atom is in a pseudo square planar environment (Pt–N1 = 2.053(4) Å; Pt–N2 = 2.056(3) Å; Pt–S4 = 2.2544(11) Å; Pt–S1 = 2.2574(12) Å; N1–Pt–N2 = 78.87(14)°; N1–Pt–S4 = 96.26(10)°; N2–Pt–S1 = 96.51(10)°; S4–Pt–S1 = 89.13(4)°). The dithiolene fragment and the bipyridine fragment are not coplanar, but slightly twisted by 16.89° around the platinum center. It can also be noticed that the ethylenic bridge of the dddt ligand is bended out of plane of the complex by 83°. The molecules are packed in a head-to-tail fashion along the  $a$  axis (Figure 1b), the best way to accommodate the bulky <sup>t</sup>Bu groups. Along the stack, bipyridine fragments exhibit a bond-over-ring overlap, preventing the formation of short platinum-platinum contacts. The shortest platinum-platinum distance along the stack is indeed 5.348 Å.

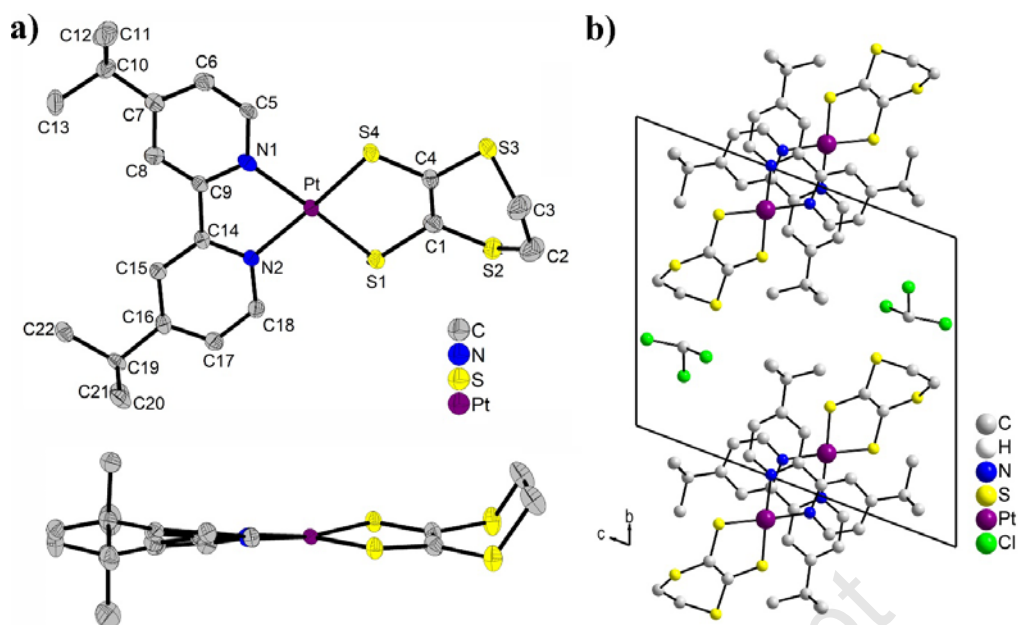


**Figure 1.** a) ORTEP diagram of **1c** from the top and from the side with 50% thermal contours for all atoms and the atomic numbering scheme. H atoms have been omitted for the sake of clarity; b) Projection of the crystalline structure along the *a* axis.

### Spectroscopic properties in solution

Spectroscopic data for all the complexes and their precursors in diluted  $\text{CH}_2\text{Cl}_2$  solutions are gathered in Table 1. The absorption spectra are presented in Figure 2a and in Figures S1-S5. The absorption spectrum of the bpyC<sub>12</sub> ligand **3a** shows a main broad absorption band exhibiting a maximum at 298 nm ( $\epsilon \sim 22450 \text{ M}^{-1}\text{cm}^{-1}$ ) with a shoulder at 338 nm (Figure S1). These absorption bands are assigned to  $\pi\text{-}\pi^*$  and  $n\text{-}\pi^*$  transitions localized on the bipyridine core and on the alkoxyphenyl fragments, respectively.<sup>[18]</sup> The absorption spectrum of the bpyCBP ligand **3b** also displays an absorption band centred at 298 nm but the band is much sharper and the associated extinction coefficient is much higher compared with **3a** (Figure 2a and S1). This absorption band is assigned to  $\pi\text{-}\pi^*$  transitions localized on the bipyridine core but also to  $\pi\text{-}\pi^*$  transitions localized on the cyanobiphenyl fragments.<sup>[19]</sup> Coordination of the  $\text{PtCl}_2$  fragment leads to a new absorption band at 412 nm for **4a** and 429 nm for **4b** (Figure S2

and 2a) with weak extinction coefficients. These absorption bands are readily associated to the charge transfer transition corresponding to excitations from a filled Pt(d) orbital to an unoccupied  $\pi^*$  diimine orbital (MLCT).<sup>[20]</sup> Introduction of the dddt<sup>2-</sup> in place of the chloride ligands is characterized in **1a** by an additional absorption band on the spectrum at even lower energy, associated to mixed metal ligand-to-ligand charge transfer transition (MMLL'CT) corresponding to excitation from the electron donor dithiolate ligand having orbital contributions from the metal ion to the electron acceptor bipyridine ligand (Figure 2a and S3).<sup>[21]</sup> With the C<sub>12</sub>dt dithiolene ligand, the position of this MMLL'CT band in **1b** is weakly affected by the nature of the bipyridine ligand and is located around 630-660 nm (Figure S4). On the contrary, with the dddt ligand, the MMLL'CT band is located at 635 nm in **1c** (Figure S5) whereas this band is red-shifted to 712 and 770 nm for **1a** and **1b**, respectively. An MLCT band is present for all the complexes and it can be noticed that with the bpyC<sub>12</sub> ligand, the MLCT band of the complexes is slightly blue-shifted compare to the bpyCBP ligand. Solid-state absorption spectra of some complexes have been measured (Figure S6). The absorption maxima are close to those measured in solution and only a broadening of the absorption bands is observed. Solids-state absorption spectra of the platinum diimine-dithiolene complexes clearly display the LLCT at low energy, showing that the charge transfer is also effective in solid-state.

The luminescence properties of all the compounds were also investigated in CH<sub>2</sub>Cl<sub>2</sub> solutions. The bpyC<sub>12</sub> diimine **3a**, its PtCl<sub>2</sub> complex **4a** and the dddt complex **1a** are non-luminescent. On the other hand, spectrum of complex **1b** with the other C<sub>12</sub>dt dithiolene ligand shows an emission band centered at 485 nm upon excitation in the MLCT band at 430 nm (Figure 2b). For all complexes carrying a bpyCBP ligand **3b**, an emission band is observed around 370 nm upon excitation at 300 nm. This emission is attributed to the presence of cyanobiphenyl fragments (Figure S6). All the other complexes show a weak luminescence upon

excitation in the MLCT band. Introduction of ester or amide functionalities on the bpy fragments (as in **3a** or **3b**) leads to a red-shift of the emission band, in line with the red-shift of the MLCT band. In fact, with the C<sub>12</sub>dt ligand, complex **2d** absorbs at 348 nm and emits at 441 nm whereas **2a** and **2b** absorb at 430 and 443 nm and emit at 485 and 520 nm, respectively (Figure 2b). The same observation can be done with the dddt ligand between **1a**, **1b** and **1c**. Introduction of the ester or the amide groups leads to the red-shift of both the MLCT and the emission bands. Comparison of two bpyCBP complexes **1b** and **2b** with respectively the dddt and C<sub>12</sub>dt dithiolene ligands shows that the nature of the dithiolate ligand affects the emission properties much more strongly. Indeed, in **1b**, the emission appears at 612 nm and is red-shifted by 92 nm when compared to **2b**. This red-shift is likely attributed to the fact that the dddt ligand is more electron rich than the C<sub>12</sub>dt ligand. No emission has been detected at room temperature upon excitation in the low energy MMLL'CT band. Thus, it appears here that the emission observed at room temperature upon excitation around 450-500 nm is only due to a <sup>3</sup>MLCT state and not to the MMLL'CT state.<sup>[13]</sup>

Quantum yields of emission of the various compounds upon excitation in the MLCT band were measured in CH<sub>2</sub>Cl<sub>2</sub> solutions (Table 1). They are always very low, between 0.1 and 1.2 %. The highest quantum yields were found with the free bipyridine **3b**. All complexes are luminescent in fluid solution at room temperature and their emission properties can be tuned through ligand variation. It can also be noticed that epifluorescence investigations on solids have revealed that the dichloroplatinum diimine complexes **4a** and **4b** show strong red and yellow luminescence at room temperature upon excitation in the range 350-380 nm, respectively, whereas all the diimine-dithiolene complexes (**1a-c**, **2a**, **2b**, **2d**) are deprived of naked-eye luminescence properties in the solid state. For complexes **4a** and **4b**, a broad emission centered at 670 and 650 nm, respectively, is observed in solid-state upon excitation at 420 nm (Figure S8).

**Table 1.** Optical data measured in CH<sub>2</sub>Cl<sub>2</sub> solution at 298 K.

<b>Compound</b>	$\lambda_{\text{abs}}$ (nm) $\varepsilon$ (M <sup>-1</sup> .cm <sup>-1</sup> )	$\lambda_{\text{ex}}$ (nm)	$\lambda_{\text{F max}}$ (nm)	$\Phi_{\text{F}}$ <sup>[a]</sup>
bpyC <sub>12</sub> <b>3a</b>	298 (22450)	298	-	-
bpyCBP <b>3b</b>	298 (55900)	298	366	Not measured
Cl <sub>2</sub> Pt(bpyC <sub>12</sub> ) <b>4a</b>	300 (28300)	300	-	-
	412 (9630)	412	-	-
Cl <sub>2</sub> Pt(bpyCBP) <b>4b</b>	300 (52600)	300	369	Not measured
	429 (3510)	429	485	0.0023
(ddd)tPt(bpyC <sub>12</sub> ) <b>1a</b>	316 (23425)	316	-	-
	414 (9060)	414	-	-
	712 (1630)	712	-	-
(ddd)tPt(bpyCBP) <b>1b</b>	300 (61230)	300	379	Not measured
	440 (3050)	440	612	0.0097
	776 (1611)	770	-	-
(C <sub>12</sub> dt)Pt(bpyC <sub>12</sub> ) <b>2a</b>	306 (72740)	306	-	-
	430 (16832)	430	485	0.0065
	626 (6900)	626	-	-
(C <sub>12</sub> dt)Pt(bpyCBP) <b>2b</b>	298 (216050)	298	373	Not measured
	443 (9187)	443	520	0.0123
	816 (12876)	640	-	-
(ddd)tPt(tBu <sub>2</sub> bpy) <b>1c</b>	300 (65220)	300	-	-
	380 (7510)	380	467	0.0033
	635 (9320)	635	-	-
(C <sub>12</sub> dt)Pt(bpy) <b>2d</b>	304 (91915)	304	-	-
	348 (34520)	348	441	0.0008
	660 (11020)	660	-	-

[a] Determined in CH<sub>2</sub>Cl<sub>2</sub> solution ( $c \sim 10^{-7}$  M) using [Ru(bpy)<sub>3</sub>]Cl<sub>2</sub> as reference ( $\Phi_{\text{F}} = 0.059$  in

CH<sub>3</sub>CN,  $\lambda_{\text{exc}} = 450$  nm).<sup>[22]</sup> All  $\Phi_{\text{F}}$  are corrected for changes in refractive index.

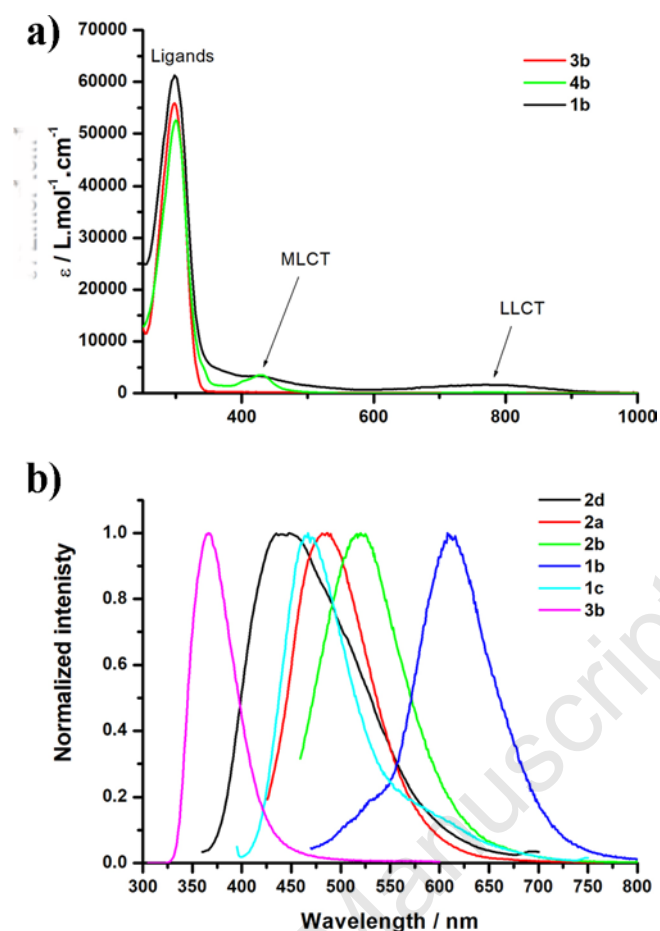


**Figure 2.** a) UV-Vis absorption spectra in  $\text{CH}_2\text{Cl}_2$  ( $C \sim 10^{-5} \text{ M}$ ) of **3b**, **4b** and **1b**; b) Normalized emission spectra in  $\text{CH}_2\text{Cl}_2$  ( $C \sim 10^{-5} \text{ M}$ ) of all the compounds upon excitation in the MLCT band (except for **3b**,  $\lambda_{\text{ex}} = 300 \text{ nm}$ ).

### Electrochemical investigations

The electrochemical behavior of complexes and their parent ligands was investigated by cyclic voltammetry in  $\text{CH}_2\text{Cl}_2$  containing 0.2 M  $n\text{Bu}_4\text{NPF}_6$  as supporting salts at 293 K. Table 2 gathers the formal potentials  $E_{1/2}$  derived as the mid-sum of oxidation ( $E_{\text{pa}}$ ) and reduction ( $E_{\text{pc}}$ ) peak potentials (relative to the SCE reference electrode). Electrochemical measurements were run in the  $[-2\text{V}/+2\text{V}]$  potential range.

Cyclic voltammogram of the bipyridine **3b** shows one irreversible reduction process at  $-1.80 \text{ V}$  (Figure S9), probably due to the reduction of cyanobiphenyl groups<sup>[23,24]</sup> No reduction

process has been detected for the bipyridine **3a** but an almost irreversible oxidation at +1.15 V, followed by an ill-defined irreversible oxidation at +1.5 V are observed (Figure S10).

After metal complexation, the two bipyridine ligands undergo two successive reversible reductions at -0.95 V and -1.47 V for **4a** (Figure S11) and at -0.85 and -1.46 V for **4b** (Figure S12). Coulometric studies through comparison with ferrocene at 293 K confirm a one-electron reduction in each case. The two reversible reduction processes correspond to the formation of the monoanion and the dianion, respectively. The electron-withdrawing effect of the ester and amide groups stabilizes the di-reduced product sufficiently to allow bulk electrogeneration of the dianion at room temperature.<sup>[25]</sup> The ester functionality has a slightly stronger electron-withdrawing effect when compared with the amide function and the **4b** complex is more easily reduced, at least in the first reduction process. The irreversible oxidation observed for **4a** (Figure S11) at +1.2 V could be attributed to the oxidation of the amide ligand.

The reference compound with the dddt ligand, **1c**, exhibits one reversible reduction at -1.45 V, assigned to a bpy ligand-based reversible reduction (Figure S13). This compound also exhibits two reversible oxidation processes at +0.24 and +1.02 V, corresponding to the formation of a monocation and a dication, respectively. Both cationic species are stable at the cyclic voltammetry timescale. These oxidation processes are assigned to dddt ligand-based reversible oxidations. It can be noticed that with the known Pt(ddd)(bpy) complex (**1d**), only one irreversible oxidation system has been observed at +0.34 V.<sup>[26]</sup> The presence of both reversible reduction and oxidation potentials clearly highlights the ambipolar character of our model compound **1c**. The cyclic voltammogram of the C<sub>12</sub>dt complex with bipyridine, **2d** also displays one reversible bpy ligand-based reduction system at -1.40 V, and two oxidation waves at +0.23 and +1.01 V, attributed to the C<sub>12</sub>dt ligand (Figure S14). The first oxidation system is reversible while the second one is only partially reversible, probably because of a possible degradation of the C<sub>12</sub>dt fragment. The oxidation potentials of the dddt and C<sub>12</sub>dt fragments are

very close but the dddt ligand is more stable toward oxidation. In conclusion, both model complexes **1c** and **2d** exhibit an ambipolar behavior.

Turning now to the four complexes **1a,b** and **2a,b**, cyclic voltammogram of **1b** shows two one-electron reversible oxidation processes located at +0.26 and +0.98 V (Figure 3). These values are very close to those observed with the dddt-containing complex **1c** and these oxidation processes can be then confidently attributed to the oxidation of the common dddt ligand. **1b** also exhibits two reversible reduction systems at -1.01V and -1.62 V, respectively (Figure 3). These values are more negatively-shifted than those found for the PtCl<sub>2</sub> precursor **4b**. This can be explained by the charge transfer that occurs between the dddt and the bpyCBP ligands, as revealed by UV-visible measurements. Through charge transfer, the bpyCBP is more electron rich and thus this fragment becomes more difficult to reduce.

With both the bpyC<sub>12</sub> and dddt ligands, complex **1a** exhibits two reversible reduction processes located at -1.08 and -1.60 V (Figure S15), showing that the reduction processes are also negatively-shifted compared to Cl<sub>2</sub>Pt precursor **4a**. However, only one irreversible oxidation at 1.10 V is observed, instead of having the expected two oxidations systems of dddt. We postulate that the bpyC<sub>12</sub> ligand oxidation might overlap with the dddt oxidation systems since we observe that the current intensity of the irreversible oxidation at +1.1 V is much higher than the current intensity associated with the first or the second reduction process.

The electrochemical activity of the C<sub>12</sub>dt dithiolene complexes **2a** and **2b** with long alkyl chains on both ligands could not be measured due to solubility issues, despite attempts in different solvents, including DMF, CH<sub>2</sub>Cl<sub>2</sub> and THF. However, in regard to the electrochemical activities of the reference compounds **2d**, **4a** and **4b**, these two compounds should likely display similar electrochemical behaviours with two reversible reduction systems around -0.9 and -1.5 V as well as two quasi-reversible oxidation processes around +0.2 and +0.9 V. To summarize, these electrochemical investigations demonstrate that the diamine-dithiolene core is indeed a very

attractive platform for preparing ambipolar compounds that can be easily and reversibly oxidized and reduced.

**Table 2.** Electrochemical data<sup>[a]</sup> for all compounds (versus ECS).

<b>Compound</b>	$E_{1/2\text{red}}$ (V)	$E_{1/2\text{ox}}$ (V)
bpyC <sub>12</sub> <b>3a</b>	/	+1.10 +1.50 ( $E_{\text{pa}}$ , irr.)
bpyCBP <b>3b</b>	-1.80 ( $E_{\text{pc}}$ irr.)	-
Cl <sub>2</sub> Pt(bpyC <sub>12</sub> ) <b>4a</b>	-0.95 -1.47	+1.20 ( $E_{\text{pa}}$ irr.)
Cl <sub>2</sub> Pt(bpyCBP) <b>4b</b>	-0.85 -1.46	/
(dddT)Pt(bpyC <sub>12</sub> ) <b>1a</b>	-1.08 -1.62	+1.10 ( $E_{\text{pa}}$ irr.)
(dddT)Pt(bpyCBP) <b>1b</b>	-1.01 -1.60	+0.26 +0.98
(C <sub>12</sub> dt)Pt(bpyC <sub>12</sub> ) <b>2a</b>	Poorly soluble	
(C <sub>12</sub> dt)Pt(bpyCBP) <b>2b</b>	Poorly soluble	
(dddT)Pt(tBu <sub>2</sub> bpy) <b>1c</b>	-1.45	+0.25 +1.03
(C <sub>12</sub> dt)Pt(bpy) <b>2d</b>	-1.40	+0.23 +1.01 ( $E_{\text{pa}}$ irr.)

[a] Determined in CH<sub>2</sub>Cl<sub>2</sub> + 0.2 M nBu<sub>4</sub>NPF<sub>6</sub> solution ( $c \sim 10^{-3}$  M) at room temperature; scan rate, 100 mVs<sup>-1</sup>.  $E_{1/2} = (E_{\text{pa}} + E_{\text{pc}})/2$ ;  $E_{\text{pa}}$  and  $E_{\text{pc}}$  are the anodic peak and the cathodic peak potentials, respectively.

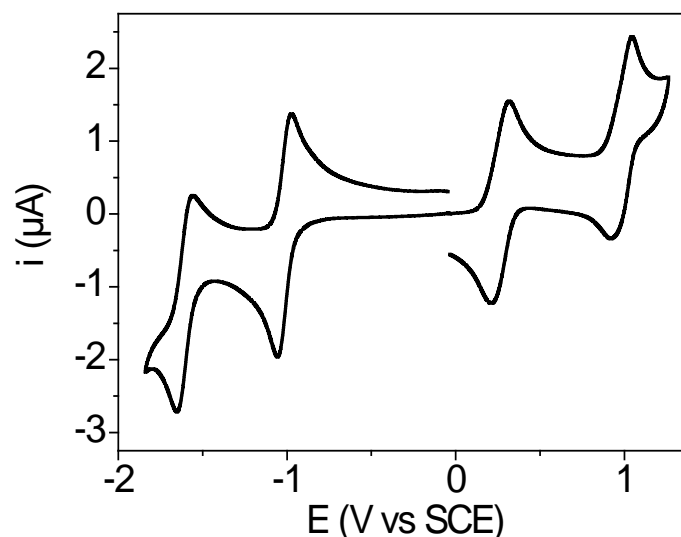


**Figure 3.** Cyclic voltammogram of (ddd)Pt(bpyCBP) **1b** ( $\sim 10^{-3}$  M) in  $\text{CH}_2\text{Cl}_2$  containing 0.2 M  $\text{NBu}_4\text{PF}_6$  at a 1-mm disk carbon electrode. Scan rate is  $0.1 \text{ V s}^{-1}$  and  $T = 293 \text{ K}$ .

### DFT calculations

In order to get more insight into the electronic properties of the newly developed diimine-dithiolene complexes, DFT geometry optimization of models of the complexes were carried out *in vacuo*. To optimize the computing time, the long carbon chains have been systematically replaced by methyl group, giving the corresponding **1a'**, **1b'**, **2a'** and **2b'** complexes. These calculations have also been conducted to estimate the energy levels and the nature of the redox-active molecular orbitals of **2a** and **2b** since both these compounds are poorly soluble and not amenable to an electrochemical study. Figure 4 shows that all calculated compounds have a HOMO level comprised between  $-4.63$  and  $-4.90$  eV and a LUMO level between  $-3.17$  and  $-3.48$  eV. Specifically, the HOMO of **2a'** (analog of insoluble **2a**) is only 0.15 eV higher than that of **1a'** while its LUMO lies 0.17 eV higher. Likewise the HOMO of **2b'** (analog of the insoluble **2b**) is also only 0.17 eV higher than that of **1b'** while its LUMO lies 0.15 eV higher. Taken together these results indicate that the oxidation potential of the  $\text{C}_{12}\text{dt}$ -ligated insoluble compounds **2a** and **2b** should be slightly higher and their reduction redox potentials slightly

lower than their dddt-ligated congeners **1a** and **1b**. Examination of the nature of the frontier molecular orbitals of the calculated models (Figure 4) shows that the HOMOs of the Pt(II) diimine-dithiolene complexes is mainly centered on the bpy ligand with a metallic character while the LUMOs is mainly centered on the dithiolene ligand also with a metallic character. Hence, from these calculations, the lowest-energy transition between the frontier orbitals is best described as a mixed metal-ligand to mixed metal-ligand charge transfer (MMLMML'CT). The HOMO-LUMO gaps were computed for all the complexes at ca. 1.45 eV *in vacuo* which would correspond to a low energy transition in the UV-visible-NIR spectra around 855 nm.

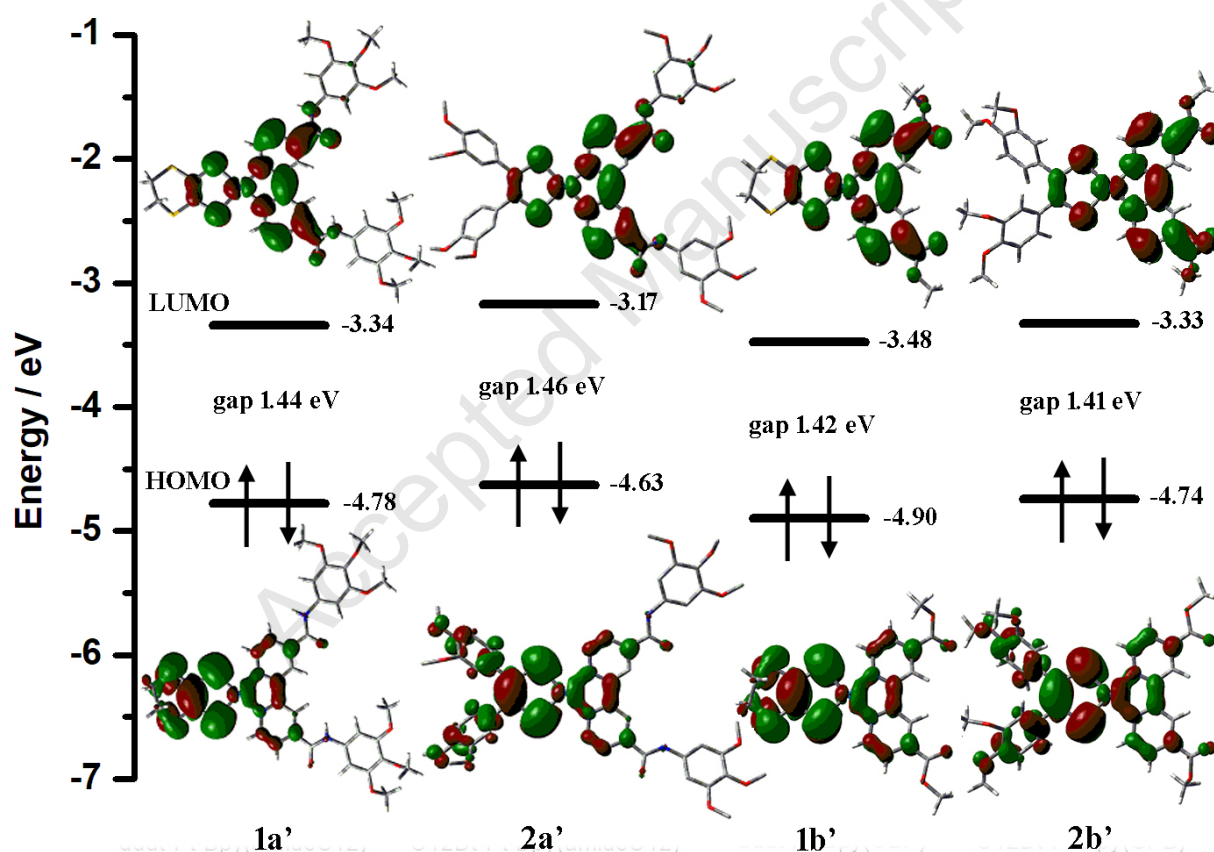
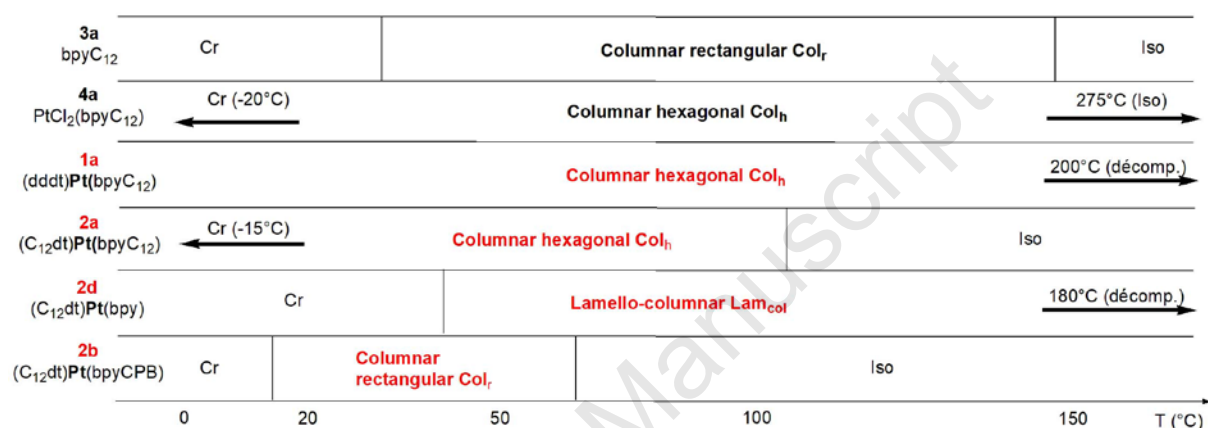


**Figure 4.** HOMO and LUMO frontier orbitals with energy levels (eV) of **1a'**, **2a'**, **1b'** and **2b'** obtained by DFT B3LYP/LANL2DZ.

### Thermal and mesomorphic properties

The thermal and mesomorphic properties of all the compounds carrying long carbon chains have been investigated by a combination of Polarized Optical Microscopy (POM), Differential Scanning Calorimetry (DSC) and Small Angle X-ray Scattering (SAXS). The transition temperatures, the enthalpies and the XRD results of all compounds are gathered in Table S5 and the thermal behaviors of the liquid crystalline compounds are summarized in the Scheme 3.



**Scheme 3.** Summary of the thermal behaviour of the liquid crystalline compounds.

The bpyC<sub>12</sub> ligand **3a** is in a mesomorphic state between 30 and 146 °C (Figure S16). On cooling from the isotropic state, a homogeneous and fluid texture develops between cross-polarizers (developable cylindrical domains) characteristic of a columnar phase (Figure S17). X-ray diffraction patterns recorded between 30 and 146 °C exhibit a series of sharp peaks in the small angle region that can be indexed as the reflections of a rectangular lattice ( $a = 54.9 \text{ \AA}$ ,  $b = 41.4 \text{ \AA}$  at 140 °C) (Figure S18). In the wide angle region, a broad halo centered at  $4.5 \text{ \AA}$ , associated to the mean distance between the alkyl chains in a molten state, confirms the liquid crystalline nature of the phase. An additional peak ( $h_{\text{stack}}$ ) centered at  $4.74 \text{ \AA}$  is also observed and is attributed to the stacking distance between the bpyC<sub>12</sub> **3a** molecules along the column axis. Using a standard geometrical treatment, it is found that the rectangular unit cell  $h_{\text{stack}}$ -thick

contains 4 molecules ( $N = S_{\text{cell}} \times h_{\text{stack}} / V_m$  with  $V_m = (M_w/0.6022)$ ).<sup>[27]</sup> Based on X-ray data, the size of the molecule and the number of molecules inserted inside the unit cell, a packing model can be proposed in which the bpyC<sub>12</sub> molecules are associated head to head to form a disc and the stacking of these dimeric discs leads to the formation of columns organized in the node of the rectangular lattice. FT-IR spectroscopic investigations performed on powder at room temperature show that the columnar organization is also stabilized by hydrogen bonding between the amide functionalities, as clearly evidenced by the  $\nu_{\text{NH}}$  and  $\nu_{\text{CO}}$  stretching vibrations observed respectively at 3246 and 1650  $\text{cm}^{-1}$  (see experimental part). Note that corresponding values for the free amide are usually found at 3400  $\text{cm}^{-1}$  for  $\nu_{\text{NH}}$  and around 1680  $\text{cm}^{-1}$  for  $\nu_{\text{CO}}$ .<sup>[28]</sup> The presence of single  $\nu_{\text{CO}}$  and  $\nu_{\text{NH}}$  stretching vibrations on the FTIR spectra also indicate the formation of a hydrogen bonded network involving all amide functionalities.

Interestingly, PtCl<sub>2</sub> complexation of the free bipyridine ligand **3a** strongly increases the thermal domain of the mesophase, from  $-20$  to  $+275^\circ\text{C}$  (Figure S19). Above  $275^\circ\text{C}$ , the dichloroplatinum complex **4a** is in an isotropic state and upon cooling, a fluid and birefringent texture with pseudo-fans shapes characteristic of columnar phases readily forms (Figure S20). Temperature-dependent XRD analyses confirm the existence of a columnar mesophase of hexagonal symmetry over the whole mesomorphic domain. The XRD patterns display in the small angle region four sharp peaks which can be unambiguously indexed as the 10, 21, 20 and 22 reflections of a 2D hexagonal lattice (Figure S21). The XRD pattern also displays a broad halo around 4.85 Å, indicative of the molten state of the alkyl chains. The hexagonal unit cell  $h_{\text{ch}}$ -thick contains 2 molecules and this also indicates that two molecules are associated inside the columnar stratum. The observation of a broad halo around 8.5 Å ( $h'_{\text{stack}}$ ) corresponding to almost two times the  $h_{\text{ch}}$  distance and of a broad halo around 3.5 Å ( $h_{\text{stack}}$ ) accounts for a head-to-tail organization of the molecules mainly driven by  $\pi$ - $\pi$  stacking. No additional absorption or emission band associated to the presence of a metal-metal-to-ligand-charge-transfer state due

to Pt-Pt interactions has been observed in solid state (Figure S6 and Figure S8).<sup>[29]</sup> So, there is no evidence of the stabilization of the supramolecular arrangement through intermolecular Pt-Pt interactions. Room temperature FT-IR measurements also confirm here ( $\nu_{\text{NH}} = 3372 \text{ cm}^{-1}$  and  $\nu_{\text{CO}} = 1672 \text{ cm}^{-1}$ , see experimental part) that the columnar organization of **4a** is stabilized by hydrogen bonding between the amide functions of the ligand **3a**.

DSC and POM investigations have shown that the dddt/bpyC<sub>12</sub> Pt complex **1a** degrades above 200 °C. No phase transition could be detected between -25 °C and +200 °C (Figure S22). Between room temperature and 200 °C, **1a** appears as a birefringent and malleable soft material (Figure S23), which is a good indication that this compound is a liquid crystalline material. The SAXS patterns shows only one clear peak in the small angle region and no clear assignment can be done (Figure S24). However, in regard to the shape of the molecule and the previous results, it can be hypothesized that this compound is also likely organized into a columnar mesophase of hexagonal symmetry stabilized through hydrogen bonding between the amide functionalities ( $\nu_{\text{NH}} = 3326 \text{ cm}^{-1}$  and  $\nu_{\text{CO}} = 1676 \text{ cm}^{-1}$ ). With this hypothesis, the single observed reflection can be tentatively assigned as the (10) reflection of a 2D hexagonal lattice. It demonstrates however that the introduction of the dddt ligand strongly destabilizes the molecular organization inside the mesophase but the temperature range of existence of the mesophase is weakly affected. All these observations clearly highlight that this compound is also a liquid crystal.

Replacing the dddt ligand in **1a** by the C<sub>12</sub>dt one gives **2a** with long alkyl chains on both ligands. **2a** is a birefringent soft material at room temperature. Upon heating, the viscosity of the compound decreases and the compound slowly become isotropic between 90 °C and 120 °C. The DSC traces display no thermal transition at 100 °C, in line with a slow isotropization process extended over a large temperature range (Figure S25). Only a broad transition, associated to the slow crystallization of the carbon chains, is observed around -15 °C.

Temperature-dependent XRD measurements confirm that the compound is isotropic above 100 °C with patterns displaying only broad halos in the whole  $2\theta$  range explored. Below 90°C, the obtained diffractions patterns, with several sharp peaks in the small angle region and a broad peak around 20° in  $2\theta$ , clearly indicates that this compound is a liquid crystalline material (Figure 5). The four sharp peaks observed at low angles can unambiguously be indexed as the (10), (11), (20) and (21) reflections of a 2D lattice of hexagonal symmetry. The broad peak ( $h_{ch}$ ) at 4.5 Å indicates that the carbon chains are in a molten state. Thus, this compound is organized from -15 °C up to 90 °C into a columnar mesophase of hexagonal symmetry. The broad halo ( $h_{stack}$ ) observed at 3.4 Å is associated with short stacking along the column ( $\pi$ - $\pi$  stacking). No evidence of Pt-Pt interactions has been detected by solid-state optical spectroscopy (Figure S6 and S8). The hexagonal unit cell  $h_{stack}$ -thick contains one molecule. So, here the columns are directly formed by a stacking of the disk-like molecules and the columns are then organized on the node of the 2D hexagonal cell with a parameter  $a$  of 41.2 Å. To compensate the dipole moment and for a better space-filling, the molecule should adopt a head-to-tail arrangement along the columnar stacks (Figure 6).

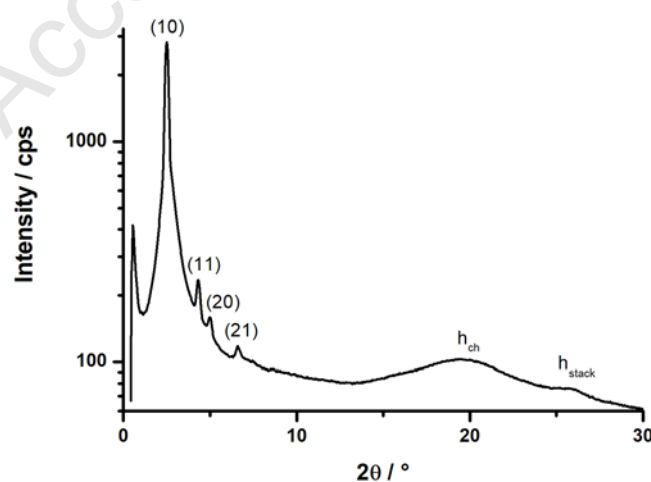


**Figure 5.** SAXS pattern of **2a** recorded at 70 °C (2<sup>nd</sup> heating).

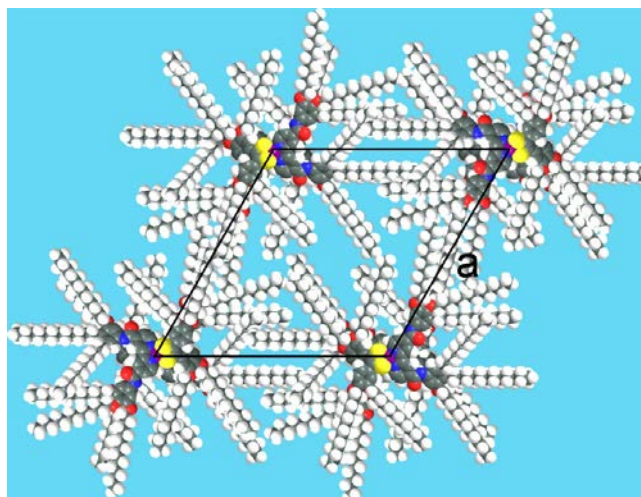


**Figure 6.** Proposed model for the organization of **2a** in the  $Col_h$  phase (Molecular diameter  $\sim 48$  Å (Dreiding model); atom: white = hydrogen, grey = carbon, blue = nitrogen, yellow = sulfur, purple = platinum, red = oxygen).

In conclusion, all the compounds incorporating the  $bpyC_{12}$  ligand **3a**, namely, **3a** itself, **4a**, **1a**, and **2a** were found to be liquid crystalline materials, highlighting that this novel ligand is a successful mesomorphic promotor of great interest to develop new metallomesogens.

DSC analyses, temperature-dependent XRD measurements and POM observations have revealed that the reference complex **2d**,  $(C_{12}dt)Pt(bpy)$  is a liquid crystalline material from 42 °C up to the decomposition temperature around 180 °C (Figure S26 and S27). All the recorded XRD diffractograms (between 60 to 180 °C) are identical, and five sharp and intense small-angle reflections with reciprocal spacings in the ratios 1:2:3:4:5 are observed (Figure S28). These small-angle peaks are most readily assigned as the (001), (002), (003), (004) and (005) reflections of a lamellar phase with an interlayer spacing parameter  $d = 32.2$  Å (at  $T = 150$  °C, Table 3). In the wide angle region, a strong sharp peak is also observed at 3.46 Å and is

associated to a strong regular stacking of the molecule into columns. The SAXS patterns also displaying two additional small reflections at 9.01 and 4.375 Å with reciprocal spacings in the ratio 1:2, which are associated to a lateral periodicity inside the plane. From the above XRD data, a model of organization can be proposed in which the molecules stack on top of each other to form columns with a periodicity of 3.46 Å and these columns are then organized at a distance of 9 Å into planes 32 Å thick. This complex is organized into a lamello-columnar mesophase from 42 °C to 180 °C. The proposed model in Figure S29 is in good agreement with the molecular dimensions but implies some interdigitations of the carbon chains (Figure S28). Below 42 °C, the XRD patterns show several sharp peaks over the whole  $2\theta$  range and this confirms the crystallization of the compound at low temperatures.

Concerning the CBP series, the diimine ligand **3b** is deprived of mesomorphic properties and this crystalline compound directly melts into an isotropic liquid around 140°C (Figure S30). Coordination with PtCl<sub>2</sub> to give **4b** did not allow for the emergence of liquid crystalline properties and only crystalline phases have been detected by SAXS. The DSC obtained with **4b**, displaying endothermic and endothermic peaks on the heating curves, is indicative of strongly hindered crystallization processes (Figure S31). DSC analyses, POM observations and X-ray analysis observations have revealed that the corresponding dddt complex **1b** is a crystalline compound which decomposes above 180 °C (Figure S32). Finally, the introduction of the C<sub>12</sub>dt dithiolene ligand carrying long carbon chains confers liquid crystalline properties to the CBP series. The DSC traces of **2b**, (C<sub>12</sub>dt)Pt(bpyCBP), obtained upon heating display two broad endothermic transitions extending from -10 to +40 °C and from +70 °C to +100 °C (Figure S33). Above 100 °C, POM observations confirm that the complex is in an isotropic state. The high temperature transition undergoes a strong supercooling effect and a fluid and birefringent film readily forms below 45 °C, indicative of a liquid crystalline state that remains

down to room temperature. No clear textural defect could have been developed, so no proper assignment of the phase symmetry can be done by POM. The low temperature transition is likely associated with slow crystallization of the complex. In the mesomorphic domains, the SAXS patterns displays several sharp peaks in the small angle region which can tentatively be indexed as the (11), (02), (22), (31) and (24) reflections of a rectangular lattice corresponding to the plane group C2mm ( $h+k = 2n$ ) ( $a = 42.8 \text{ \AA}$ ,  $b = 42.5 \text{ \AA}$  at  $30 \text{ }^\circ\text{C}$ ) (Figure 7). Two broad peaks are also observed in the wide angle region at 5.6 and 4.4 and are attributed to the mean distance between the CBP fragments and the carbon chains, respectively.<sup>[19]</sup> A last broad peak is also observed at  $3.4 \text{ \AA}$  and is attributed to the stacking distance between the disk molecules. Applying the standard geometrical treatment, it is found that two molecules of **2b** are contained inside a unit cell  $h_{\text{stack}}$  thick, as expected for a rectangular cell. From the XRD data, an organization model can be proposed in which the molecules are stacked on top of each other to form columns and these columns are then organized on the two nodes of the 2D rectangular lattice (Figure 8). For a space filling, these dissymmetric disk-like molecules are certainly arranged head-to-tail with no obvious segregation between the cyanobiphenyl fragment and the carbon chains. To summarize, in the CBP series, only complex **2b** forms a columnar mesophase of rectangular symmetry from 40 to 70  $^\circ\text{C}$  on heating and from 40 to 20  $^\circ\text{C}$  upon cooling. With the CBP ligand, it is mandatory to introduce long carbon chains on the other side of the molecule (as in **2b**) to give it a disk-like shape able to organize into a mesophase.

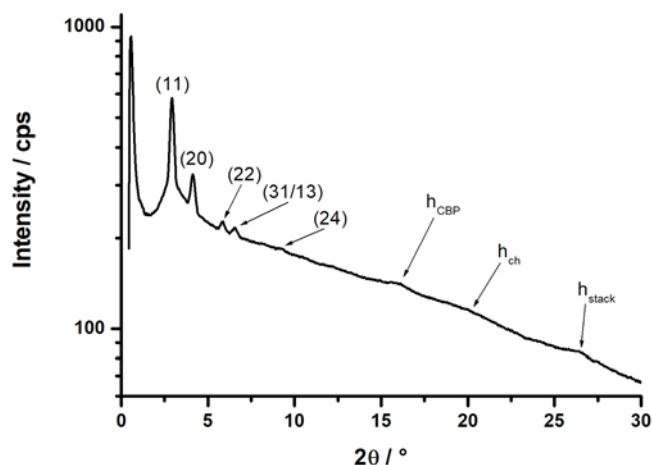


**Figure 7.** XRD pattern of **2b**, (C<sub>12</sub>dt)Pt(bpyCBP), recorded at 30 °C after cooling from the isotropic phase.

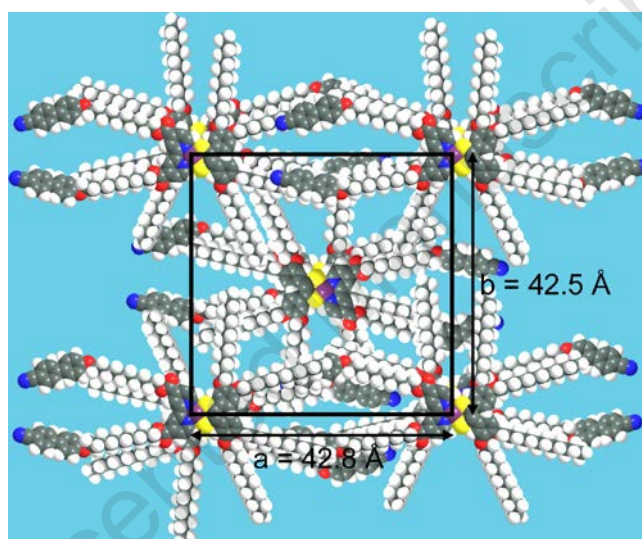


**Figure 8.** Proposed organization for **2b** in the rectangular unit cell  $h_{\text{stack}}$  thick ( $h_{\text{stack}} = 3.6 \text{ \AA}$ ) (extended length  $\sim 53 \text{ \AA}$  (Dreiding model)); atom: white = hydrogen, grey = carbon, blue = nitrogen, yellow = sulfur, purple = platinum, red = oxygen).

In the bpyC12 series, all the compounds were found to be liquid crystalline materials with columnar mesophase of hexagonal or rectangular symmetry, meaning that bpyC12 ligand is a very good mesogenic promotor. On the contrary, with the bpyCBP ligand, liquid crystalline properties could be obtained provided that numerous long carbon chains were introduced on

the dithiolate ligand to make the molecule more disk-shape and to counter-balance the stacking/crystallization of the cyanobiphenyl fragments.

## Conclusion

Highly functional platinum diimine-dithiolene complexes have been isolated through an original synthetic route based on ligand metathesis. For this purpose, novel functional bipyridines carrying either tris-dodecyloxyphenyl fragments connected through an amide linker (bpyC<sub>12</sub>) or cyanobiphenyl fragments connected through ester linker carrying a C<sub>10</sub> carbon chain (bpyCBP) have been developed. After coordination to PtCl<sub>2</sub>, the chlorine ligands have been successfully exchanged by dddt or C<sub>12</sub>dt dithiolene ligands directly from preformed tin or nickel dithiolene complexes. Thermal and X-ray analyses have revealed that, with the bpyC<sub>12</sub> diimine ligand, columnar mesophase can be obtained over a large temperature range, showing that this ligand is a good mesogenic promoter. On the contrary, with the bpyCBP diimine ligand, it was mandatory to introduce numerous long carbon chains on the dithiolene fragment to observe the emergence of liquid crystalline properties. Inside the mesophase, the platinum diimine-dithiolene complexes are stacked in a head-to-tail fashion to form columns and these columns are then organized on the nodes of the 2D lattices or into lamellas. Charge transfer occurs from the electron donor dithiolate ligand to the electron acceptor bipyridine, as revealed the additional absorption band on the spectrum at low energy around 600-800 nm, depending on the nature of the ligands. The ambipolar character of these compounds was unambiguously confirmed by electrochemical investigation coupled to DFT calculations. In fact, the liquid crystalline platinum diimine-dithiolene complexes can be oxidized and reduced at easily accessible potentials. In particular, the platinum compound **2d** with the dddt and the bpyC<sub>12</sub> ligands can clearly be reversibly oxidized or reduced and self-assembles into a lamello-columnar phase over a large temperature range from 42 °C up to 180 °C. Such ambipolar and

liquid crystalline platinum diimine-dithiolene complexes are good candidates to develop new semiconducting soft materials and this work paves the way to develop new active layers in optoelectronic devices.

### **Experimental part.**

300 ( $^1\text{H}$ ) and 75.5 MHz ( $^{13}\text{C}$ ) NMR spectra were recorded on Bruker Avance 300 spectrometer at room temperature using perdeuterated solvents as internal standards. FT-IR spectra were recorded using a Bruker VERTEX 70 spectrometer equipped with an ATR apparatus. Elemental analyses were performed by the Service de Microanalyse, Institut de Chimie des Substances Naturelles, Gif sur Yvette, France. Mass spectra were recorded with a MALDI-TOF Microflex LT Bruker. UV-Vis spectra were recorded using a Cary 100 UV-Vis spectrophotometer (Varian). Photoluminescence spectra in solution were recorded with a Jobin-Yvon spectrofluorimeter. Quantum yields in solution ( $\phi_{\text{sol}}$ ) were calculated relative to  $\text{Ru}(\text{bpy})_3\text{Cl}_2$  ( $\phi = 0.059$  in  $\text{CH}_3\text{CN}$ ).  $\phi_{\text{sol}}$  was determined according to the following equation,

$$\phi_{\text{sol}} = \phi_{\text{ref}} \times 100 \times [(T_s \times A_r)/(T_r \times A_s)] \times [(n_s/n_r)^2]$$

where, subscripts s and r refer respectively to the sample and reference. The integrated area of the emission peak in arbitrary units is given as T, n is the refracting index of the solvent ( $n = 1.3404$  for acetonitrile,  $n = 1.4242$  for  $\text{CH}_2\text{Cl}_2$  and  $n = 1.4305$  for DMF) and A is the absorbance.

Differential scanning calorimetry (DSC) was carried out by using NETZSCH DSC 200 F3 instrument equipped with an intracooler. DSC traces were measured at  $10\text{ }^\circ\text{C}/\text{min}$  down to  $-25\text{ }^\circ\text{C}$ .

Optical microscopy investigations were performed on a Nikon H600L polarizing microscope equipped with a Linkam "liquid crystal pro system" hotstage LTS420. The microscope is also

equipped with a UV irradiation source (Hg Lamp,  $\lambda = 340\text{-}380\text{ nm}$ ) and an ocean optic USB 2000+ UV-Vis-NIR spectrophotometer based on CCD detection technology.

X-ray scattering experiments (SAXS) were performed using a FR591 Bruker AXS rotating anode X-ray generator operated at 40 kV and 40 mA with monochromatic Cu K $\alpha$  radiation ( $\lambda = 1.541\text{ \AA}$ ) and point collimation. The patterns were collected with a Mar345 Image-Plate detector (Marresearch, Norderstedt, Germany). The samples were held in Lindeman glass capillaries (1 mm diameter). The capillaries were placed inside a Linkam HFX350-Capillary X-Ray stage which allow measurements from  $-196\text{ }^{\circ}\text{C}$  up to  $350\text{ }^{\circ}\text{C}$  with an accuracy of  $0.1\text{ }^{\circ}\text{C}$ .

Cyclic voltammetry measurements were performed with a SP-50 biologic or a PGSTAT 302N (Eco-Chemie B.V.) potentiostat in a three-electrode glass cell. The working electrode was a 1 mm diameter glassy carbon disk and the counter electrode was a platinum wire. All reported potentials are referred to KCl Saturated Calomel Electrode (SCE) (uncertainty  $\pm 5\text{ mV}$ ). Tetra-n-butylammonium hexafluorophosphate  $\text{Bu}_4\text{NPF}_6$  was purchased from Fluka (puriss, electrochemical grade) and was used, as received, at  $0.2\text{ mol L}^{-1}$  as supporting electrolyte in anhydrous  $\text{CH}_2\text{Cl}_2$ . All electrochemical measurements were carried out inside a Faraday cage, at room temperature ( $20 \pm 2\text{ }^{\circ}\text{C}$ ) and under constant argon flow. Prior to electrochemical analyses, the working electrode was carefully polished with diamond paste (Struers) onto a  $1\text{ }\mu\text{m}$  paper cloth (Struers) and thoroughly rinsed.

For the X-ray crystal structure of complex **1c**, data were collected on an D8 VENTURE Bruker AXS diffractometer operating with graphite-monochromated Mo-K $\alpha$  radiation ( $\lambda = 0.71073\text{ \AA}$ ). The structures was solved by direct methods using the SIR92 program<sup>[30]</sup> and then refined with full-matrix least-square methods based on F2 (SHELXL-2014/7)<sup>[31]</sup> with the aid of the WINGX

program.<sup>[32]</sup> All non-hydrogen atoms were refined with anisotropic atomic displacement parameters. All H atoms have been found in the electron density maps and refined in their idealized position using the AFIX instructions. Crystallographic data on X-ray data collection and structure refinements are given in Table S2-S6. Crystallographic data for structural analysis of the complex **1c** has been deposited with the Cambridge Crystallographic Data Centre under CCDC 1867102. Copies of this information is available free of charge from the Web site ([www.ccdc.cam.ac.uk](http://www.ccdc.cam.ac.uk)).

Density Functional Theory<sup>[33]</sup> calculations were performed with the hybrid Becke-3 parameter exchange functional<sup>[34]</sup> and the Lee-Yang-Parr nonlocal correlation functional<sup>[35]</sup> (B3LYP) implemented in the Gaussian 09 (Revision B.01) program suite<sup>[36]</sup> using the pseudo-potentials LANL2DZ with the default convergence criteria implemented in the program. Calculations were carried out on the OCCIGEN calculator of the Centre Informatique National de l'Enseignement Supérieur (CINES (Montpellier) under project 2018-A0040805032). Figures were generated with GaussView 5.0.

## Synthesis.

[2,2'-bipyridine]-4,4'-dicarboxylic acid<sup>[37]</sup>, 3,4,5-tris(dodecyloxy)aniline<sup>[38]</sup> Bis[1,2-bis(3',4'-di-n-dodecyloxyphenyl)ethane-1,2dithiolene]nickel (complex **6**),<sup>[39]</sup> 4'-[(10-bromodecyl)oxy]-4-carbonitrile-[1,1'-Biphenyl],<sup>[40]</sup> Dichloro(4,4'-di-ter/-butyl-2,2'-bipyridine)platinum(II) ([PtCl<sub>2</sub>(<sup>t</sup>bu<sub>2</sub>bpy)) (complex **4c**),<sup>[41]</sup> Dichloro(2,2'-bipyridine)platinum(II) ([PtCl<sub>2</sub>(bpy)]) (complex **4d**),<sup>[41]</sup> 2,2-Dibutyl-5,6-dihydro-1,3,2-dithiastannolo[4,5-b][1,4]dithiin (complex **5**),<sup>[42]</sup> PtCl<sub>2</sub>(DMSO)<sub>2</sub><sup>[43]</sup> were synthesized as

previously described. All the other reagents were purchased from commercial sources and used as received. All synthetic manipulations were performed under an inert and dry nitrogen atmosphere using standard techniques. The reactions were followed by Thin Layer Chromatography (TLC) plates, revealed with a UV-lamp at 254 nm or iodine. Silica gel used in chromatographic separations was obtained from Acros Organics (Silica Gel, ultra-pure, 40-60  $\mu\text{m}$ ). Aluminium oxide 90 standardized from Merck KGaA was also used for chromatographic separations.

### 1. Ligand 3a

[2,2'-bipyridine]-4,4'-dicarboxylic acid (0.1 g, 0.4 mmol) was first refluxed overnight in 10 mL freshly distilled  $\text{SOCl}_2$  at 90  $^\circ\text{C}$  under  $\text{N}_2$  with 1 drop of  $\text{Et}_3\text{N}$ . After removal of the excess  $\text{SOCl}_2$  and drying, the residue was dissolved in 20 mL of dry  $\text{CH}_2\text{Cl}_2$  with 3,4,5-tris(dodecyloxy)aniline (0.58 g, 0.9 mmol) and  $\text{Et}_3\text{N}$  (0.3 mL, 2.2 mmol) were added. The mixture was stirred at room temperature under  $\text{N}_2$  for 24h. The organic phase was washed with water (3x40 mL) and dried over  $\text{MgSO}_4$ . The product was purified by column chromatography on alumina using a 50/50 petroleum ether/chloroform mixture as eluent. After recrystallization in a  $\text{CH}_2\text{Cl}_2/\text{MeOH}$  mixture, the product was isolated as a white powder in 40 % yield (0.25 g).  $^1\text{H}$  NMR (300 MHz, Chloroform-*d*)  $\delta$  8.86 (d,  $J = 5.0$  Hz, 2H,  $\text{CH}_{\text{bpy}}$ ), 8.77 (s, 2H, NH), 8.41 (s, 2H,  $\text{CH}_{\text{bpy}}$ ), 7.92 (d,  $J = 4.6$  Hz, 2H,  $\text{CH}_{\text{bpy}}$ ), 7.00 (s, 4H, CH), 4.17 – 3.84 (m, 12H,  $\text{OCH}_2$ ), 1.90 – 1.54 (m, 12H,  $\text{CH}_2$ ), 1.55 – 0.97 (m, 108H,  $\text{CH}_2$ ), 0.95 – 0.80 (m, 18H,  $\text{CH}_3$ ).  $^{13}\text{C}$  NMR (75 MHz, Chloroform-*d*)  $\delta$  163.48 (Cq), 156.14 (Cq), 153.43 (Cq), 150.47 (CH), 143.58 (Cq), 135.66 (Cq), 132.94 (Cq), 122.55 (CH), 117.53 (CH), 99.53 (CH), 73.72 ( $\text{OCH}_2$ ), 69.34 ( $\text{OCH}_2$ ), 32.11 ( $\text{CH}_2$ ), 32.09 ( $\text{CH}_2$ ), 30.47 ( $\text{CH}_2$ ), 29.93 ( $\text{CH}_2$ ), 29.91 ( $\text{CH}_2$ ), 29.87 ( $\text{CH}_2$ ), 29.82 ( $\text{CH}_2$ ), 29.80 ( $\text{CH}_2$ ), 29.60 ( $\text{CH}_2$ ), 29.56 ( $\text{CH}_2$ ), 29.53 ( $\text{CH}_2$ ), 26.31 ( $\text{CH}_2$ ), 26.27 ( $\text{CH}_2$ ), 22.85 ( $\text{CH}_2$ ), 14.27 ( $\text{CH}_3$ ). IR-ATR ( $\text{cm}^{-1}$ ): 3246 ( $\nu\text{NH}$ ), 3064 ( $\nu\text{CH}$ ), 2916 ( $\nu\text{CH}$ ), 2851 ( $\nu\text{CH}$ ), 1650

( $\nu\text{C=O}$ ), 1602 ( $\nu\text{C=C}$ ), 1539 ( $\delta\text{NH}$ ), 1507 ( $\nu\text{C=C}$ ), 1464 ( $\delta\text{CH}_2$ ), 1426 ( $\delta\text{CH}_2$ ), 1386 ( $\delta\text{CH}_3$ ), 1312 ( $\nu\text{C-N}$ ), 1232, 1119, 1066, 997, 954, 911, 853, 812, 712, 657, 614, 517. UV-vis UV-vis [ $\text{CH}_2\text{Cl}_2$ ,  $\lambda_{\text{max}}$  (nm) ( $\epsilon$  ( $\text{M}^{-1}\cdot\text{cm}^{-1}$ ))]: 298 (22500). MALDI-TOF-MS:  $m/z$  = 1500.5 ( $\text{M}^+$ ). Anal. Calc. for  $\text{C}_9\text{H}_{162}\text{N}_4\text{O}_8$  (%): C 76.85, H 10.88, N 3.73. Found (%): C 76.60, H 10.98, N 3.52.

## 2. Ligand 3b

[2,2'-Bipyridine]-4,4'-dicarboxylic acid (0.12 g, 0.5 mmol) was first refluxed overnight in 10 mL freshly distilled  $\text{SOCl}_2$  at 90 °C under  $\text{N}_2$ . After removal of the excess  $\text{SOCl}_2$  by distillation and drying, the residue was dissolved in 20 mL of dry  $\text{CH}_2\text{Cl}_2$  together with 4'-[(10-bromodecyl)oxy]-4-carbonitrile-[1,1'-Biphenyl] (0.3 g, 0.9 mmol).  $\text{Et}_3\text{N}$  (0.3 mL, 2.2 mmol) was added and the reaction mixture was stirred at room temperature for 3 days. After removal of the solvent, the residue was purified by column chromatography on alumina gel using a gradient of eluents for pure  $\text{CH}_2\text{Cl}_2$  to  $\text{CH}_2\text{Cl}_2$ +1 %v/v MeOH. The product was isolated as a white powder in 56 % yield (0.25 g).

$^1\text{H}$  NMR (300 MHz, Chloroform- $d$ )  $\delta$  8.95 (s, 2H,  $\text{CH}_{\text{bpy}}$ ), 8.86 (d,  $J$  = 5.0 Hz, 2H,  $\text{CH}_{\text{bpy}}$ ), 7.89 (dd,  $J$  = 5.0, 1.6 Hz, 2H,  $\text{CH}_{\text{bpy}}$ ), 7.74 – 7.59 (m, 8H,  $\text{CH}_{\text{biph}}$ ), 7.57 – 7.43 (m, 4H,  $\text{CH}_{\text{biph}}$ ), 7.09 – 6.88 (m, 4H,  $\text{CH}_{\text{biph}}$ ), 4.39 (t,  $J$  = 6.8 Hz, 4H,  $\text{OCH}_2$ ), 4.00 (t,  $J$  = 6.5 Hz, 4H,  $\text{OCH}_2$ ), 1.96 – 1.70 (m, 8H,  $\text{CH}_2$ ), 1.69 – 1.18 (m, 24H,  $\text{CH}_2$ ).  $^{13}\text{C}$  NMR (75 MHz, Chloroform- $d$ )  $\delta$  165.34 (Cq), 159.94 (Cq), 156.67 (Cq), 150.22 (CH), 145.42 (Cq), 139.17 (Cq), 132.69 (CH), 131.41 (Cq), 128.45 (CH), 127.20 (CH), 123.37 (CH), 120.71 (CH), 119.23 (Cq), 115.23 (CH), 110.20 (Cq), 68.30 ( $\text{OCH}_2$ ), 66.18 ( $\text{OCH}_2$ ), 29.59 ( $\text{CH}_2$ ), 29.55 ( $\text{CH}_2$ ), 29.47 ( $\text{CH}_2$ ), 29.35 ( $\text{CH}_2$ ), 28.76 ( $\text{CH}_2$ ), 26.16 ( $\text{CH}_2$ ), 26.06 ( $\text{CH}_2$ ). IR-ATR ( $\text{cm}^{-1}$ ): 3065 ( $\nu\text{CH}$ ), 2918 ( $\nu\text{CH}$ ), 2850 ( $\nu\text{CH}$ ), 2221 ( $\nu\text{CN}$ ), 1725 ( $\nu\text{C=O}$ ), 1600 ( $\nu\text{C=C}$ ), 1554, 1530, 1494 ( $\nu\text{C=C}$ ), 1467 ( $\delta\text{CH}_2$ ), 1428 ( $\delta\text{CH}_2$ ), 1394, 1366, 1314, 1289, 1270, 1252, 1176, 1133, 1117, 1063, 1042, 1028, 1011, 997, 950, 920, 854, 823, 808, 768, 724, 693, 665, 616, 583, 563, 531, 510, 472, 424, 407. UV-vis [ $\text{CH}_2\text{Cl}_2$ ,

$\lambda_{\max}$  (nm) ( $\epsilon$  ( $M^{-1}\cdot\text{cm}^{-1}$ )): 298 (55900). MALDI-TOF-MS:  $m/z = 911.8$  ( $M^+$ ). Anal. Calc. for  $C_{58}H_{62}N_4O_6$ ,  $CH_3OH$  (%): C 75.13, H 7.05, N 5.94. Found (%): C 75.68, H 6.83, N 5.72.

### 3. Complex 4a

Ligand **3a** (0.1g, 0.07 mmol) was dissolved in 10 mL dry THF in a Schlenk flask with 1 eq. of  $PtCl_2(DMSO)_2$  (0.028 g, 0.07 mmol) and the reaction mixture was then heated at 60 °C for 24h. After removal of the solvent, the product was purified by column chromatography on alumina gel using chloroform as eluent. After recrystallization in a  $CH_2Cl_2/MeOH$  solvent mixture, the product was isolated as an orange powder in 76 % yield (0.09 g).

$^1H$  NMR (300 MHz, Chloroform-*d*)  $\delta$  9.38 (s, 4H, NH/ $CH_{\text{bpy}}$ ), 8.47 (s, 2H,  $CH_{\text{bpy}}$ ), 7.88 (s, 2H,  $CH_{\text{bpy}}$ ), 7.11 (s, 4H,  $CH_{\text{ph}}$ ), 4.17 – 3.65 (m, 12H,  $OCH_2$ ), 1.88 – 1.59 (m, 12H,  $CH_2$ ), 1.55 – 1.08 (m, 108H,  $CH_2$ ), 1.02 – 0.74 (m, 18H,  $CH_3$ ).  $^{13}C$  NMR (75 MHz, Chloroform-*d*)  $\delta$  162.17 (Cq), 156.44 (Cq), 153.22 (Cq), 149.38 (CH), 135.60 (Cq), 133.78(Cq), 133.26(Cq), 122.21 (CH), 107.62 (CH), 99.60 (CH), 73.84 ( $OCH_2$ ), 69.27 ( $OCH_2$ ), 32.10 ( $CH_2$ ), 30.53 ( $CH_2$ ), 30.00 ( $CH_2$ ), 29.97 ( $CH_2$ ), 29.94 ( $CH_2$ ), 29.91 ( $CH_2$ ), 29.88 ( $CH_2$ ), 29.76 ( $CH_2$ ), 29.62 ( $CH_2$ ), 29.57 ( $CH_2$ ), 26.38 ( $CH_2$ ), 26.34 ( $CH_2$ ), 22.85 ( $CH_2$ ), 14.25 ( $CH_3$ ). IR-ATR ( $\text{cm}^{-1}$ ): 3372 ( $\nu\text{NH}$ ), 3075 ( $\nu\text{CH}$ ), 2921 ( $\nu\text{CH}$ ), 2852 ( $\nu\text{CH}$ ), 1672 ( $\nu\text{C=O}$ ), 1606 ( $\nu\text{C=C}$ ), 1538 ( $\delta\text{NH}$ ), 1505 ( $\nu\text{C=C}$ ), 1467( $\delta\text{CH}_2$ ), 1421( $\delta\text{CH}_2$ ), 1383( $\delta\text{CH}_3$ ), 1347( $\delta\text{CH}_3$ ), 1307 ( $\nu\text{C-N}$ ), 1259, 1231, 1174, 1113, 1017, 908, 835, 814, 754, 721, 702, 662, 626, 589, 415. UV-vis [ $CH_2Cl_2$ ,  $\lambda_{\max}$  (nm) ( $\epsilon$  ( $M^{-1}\cdot\text{cm}^{-1}$ ))]: 412 (9300), 320 (19100), 292 (28300). MALDI-TOF-MS:  $m/z = 1728.5$  ( $M^+-Cl$ ). Anal. Calc. for  $C_{96}H_{162}Cl_2N_4O_8Pt$ , 0.5  $CH_2Cl_2$  (%): C 64.08, H 9.08, N 3.10. Found (%): C 63.79, H 8.83, N 2.90.

### 4. Complex 4b

Ligand **3b** (0.18 g, 0.2 mmol) was dissolved in 10 mL dry THF in a Schlenk flask with 1 eq. of  $\text{PtCl}_2(\text{DMSO})_2$  (0.08 g, 0.2 mmol) and the reaction mixture was then heated at 60 °C for 48h. After removal of the solvent and purification by column chromatography on alumina gel using  $\text{CH}_2\text{Cl}_2$  as eluent, the product was isolated as a yellow powder in 52 % yield (0.12 g).

$^1\text{H}$  NMR (300 MHz, Chloroform-*d*)  $\delta$  9.94 (dd,  $J = 6.0, 0.6$  Hz, 2H,  $\text{CH}_{\text{bpy}}$ ), 8.58 (d,  $J = 1.4$  Hz, 2H,  $\text{CH}_{\text{bpy}}$ ), 8.08 (dd,  $J = 6.0, 1.8$  Hz, 2H,  $\text{CH}_{\text{bpy}}$ ), 7.72 – 7.59 (m, 8H,  $\text{CH}_{\text{biph}}$ ), 7.52 (dd,  $J = 8.8, 3.0$  Hz, 4H,  $\text{CH}_{\text{biph}}$ ), 7.02 – 6.93 (m, 4H,  $\text{CH}_{\text{biph}}$ ), 4.47 (t,  $J = 6.8$  Hz, 4H,  $\text{OCH}_2$ ), 4.00 (td,  $J = 6.5, 1.5$  Hz, 4H,  $\text{OCH}_2$ ), 1.93 – 1.74 (m, 8H,  $\text{CH}_2$ ), 1.66 – 1.22 (m, 24H,  $\text{CH}_2$ ).  $^{13}\text{C}$  NMR (75 MHz, Chloroform-*d*)  $\delta$  163.11 (Cq), 159.92 (Cq), 157.34 (Cq), 145.35 (CH), 140.55 (Cq), 132.71 (CH), 131.42 (Cq), 128.46 (CH), 127.20 (CH), 122.97 (CH), 121.41 (CH), 119.24 (Cq), 115.23 (CH), 110.24 (Cq), 68.32 ( $\text{OCH}_2$ ), 67.58 ( $\text{OCH}_2$ ), 29.55 ( $\text{CH}_2$ ), 29.33 ( $\text{CH}_2$ ), 28.66 ( $\text{CH}_2$ ), 26.20 ( $\text{CH}_2$ ), 26.02 ( $\text{CH}_2$ ). IR-ATR ( $\text{cm}^{-1}$ ): 3071 (vCH), 2925 (vCH), 2852 (vCH), 2223 (vCN), 1729 (vC=O), 1601 (vC=C), 1580, 1554, 1524, 1494 (vC=C), 1472 ( $\delta\text{CH}_2$ ), 1413 ( $\delta\text{CH}_2$ ), 1289, 1248, 1180, 1142, 1116, 1062, 1031, 1013, 999, 959, 905, 874, 855, 821, 805, 762, 729, 708, 661, 564, 531, 421. UV-vis [ $\text{CH}_2\text{Cl}_2$ ,  $\lambda_{\text{max}}$  (nm),  $\epsilon$  ( $\text{M}^{-1}\cdot\text{cm}^{-1}$ ): 429 (7020), 300 (105200). MALDI-TOF-MS:  $m/z = 1140.8$  ( $\text{M}^+-\text{Cl}$ ). Anal. Calc. for  $\text{C}_{58}\text{H}_{62}\text{Cl}_2\text{N}_4\text{O}_6\text{Pt}$ ,  $\text{C}_7\text{H}_8$  (%): C 61.51, H 5.56, N 4.41. Found (%): C 61.75, H 5.91, N 4.23.

## 5. Complex 1a

Complex **4a** (0.05 g, 0.03 mmol) and one equivalent of 2,2-Dibutyl-5,6-dihydro-1,3,2-dithiastannolo[4,5-b][1,4]dithiin (0.012 g, 0.03 mmol) were dissolved in 5 mL acetone and 1 mL THF. The mixture was stirred at room temperature under air for 3 days. The green precipitate, which has formed, was filtered, washed with acetone and dried. The product was recrystallized by slow evaporation of  $\text{CH}_2\text{Cl}_2$  from a  $\text{CH}_2\text{Cl}_2/\text{CH}_3\text{CN}$  solvent mixture. After filtration and drying, the product was isolated as a green powder is 75 % yield (0.04 g).

$^1\text{H}$  NMR (300 MHz, Chloroform-*d*)  $\delta$  10.02 (s, 2H, NH), 9.13 (s, 2H,  $\text{CH}_{\text{bpy}}$ ), 7.70 (s, 2H,  $\text{CH}_{\text{bpy}}$ ), 7.26 (s, 4H,  $\text{CH}_{\text{ph}}$ ), 6.88 (d,  $J = 6.3$  Hz, 2H,  $\text{CH}_{\text{bpy}}$ ), 4.28 – 3.51 (m, 16H,  $\text{SCH}_2/\text{OCH}_2$ ), 2.07 – 1.65 (m, 12H,  $\text{CH}_2$ ), 1.65 – 0.99 (m, 108H,  $\text{CH}_2$ ), 1.06 – 0.73 (m, 18H,  $\text{CH}_3$ ).  $^{13}\text{C}$  NMR (75 MHz, Chloroform-*d*)  $\delta$  164.22 (Cq), 153.22 (Cq), 147.13 (Cq), 134.03 (Cq), 120.18 (Cq), 103.03 (Cq), 100.22 (CH), 73.80 ( $\text{OCH}_2$ ), 69.34 ( $\text{OCH}_2$ ), 32.37 ( $\text{CH}_2$ ), 30.87 ( $\text{CH}_2$ ), 30.22 ( $\text{CH}_2$ ), 30.12 ( $\text{CH}_2$ ), 29.82 ( $\text{CH}_2$ ), 26.72 ( $\text{CH}_2$ ), 23.08 ( $\text{CH}_2$ ), 14.27 ( $\text{CH}_3$ ). All the aromatic peaks are not visible on the  $^{13}\text{C}$  NMR spectrum. IR-ATR ( $\text{cm}^{-1}$ ): 3326 ( $\nu\text{N-H}$ ), 3073 ( $\nu\text{CH}$ ), 2920 ( $\nu\text{CH}$ ), 2852 ( $\nu\text{CH}$ ), 1676 ( $\nu\text{C=O}$ ), 1606 ( $\nu\text{C=C}$ ), 1546 (NH), 1504 ( $\nu\text{C=C}$ ), 1467 ( $\delta\text{CH}_2$ ), 1427 ( $\delta\text{CH}_2$ ), 1381 ( $\delta\text{CH}_3$ ), 1346 ( $\delta\text{CH}_3$ ), 1308 ( $\nu\text{C-N}$ ), 1259, 1232, 1113, 1016, 912, 806, 754, 721, 669, 624, 582. UV-vis UV-vis [ $\text{CH}_2\text{Cl}_2$ ,  $\lambda_{\text{max}}$  (nm) ( $\epsilon$  ( $\text{M}^{-1}\cdot\text{cm}^{-1}$ ))]: 414 (9060), 316 (23400). MALDI-TOF-MS:  $m/z = 1874.5$  ( $\text{M}^+$ ). Anal. Calc. for  $\text{C}_{100}\text{H}_{166}\text{N}_4\text{O}_8\text{PtS}_4$  (%): C 64.03, H 8.92, N 2.99. Found (%): C 63.64, H 9.28, N 3.01.

## 6. Complex 1c

100 mg of  $[\text{PtCl}_2(\text{t}^{\text{bu}}_2\text{bpy})]$  were dissolved with one equivalent of 2,2-Dibutyl-5,6-dihydro-1,3,2-dithiastannolo[4,5-b][1,4]dithiin (0.012 g, 0.03 mmol) in 10 mL acetone. The solution was stirring at room temperature under  $\text{N}_2$  during 20 h. After evaporation of the solvent, the product was purified by column chromatography on silica gel using a gradient of solvent from pure petroleum ether to pure  $\text{CH}_2\text{Cl}_2$ . The blue product was dissolved in  $\text{CHCl}_3$  and recrystallized by slow diffusion of pentane. 65 mg of dark-blue crystals, suitable for XRD analysis, have been isolated (54 % yield).

$^1\text{H}$  NMR (300 MHz, Chloroform-*d*)  $\delta$  8.92 (d,  $J = 6.1$  Hz, 2H,  $\text{CH}_{\text{bpy}}$ ), 7.90 (d,  $J = 2.0$  Hz, 2H,  $\text{CH}_{\text{bpy}}$ ), 7.39 (dd,  $J = 6.1, 2.0$  Hz, 2H,  $\text{CH}_{\text{bpy}}$ ), 3.03 (s, 4H,  $\text{SCH}_2$ ), 1.44 (s, 18H,  $\text{CH}_3$ ).  $^{13}\text{C}$  NMR (75 MHz, Chloroform-*d*)  $\delta$  162.84 (Cq), 155.62 (Cq), 148.35 (CH), 124.89 (CH), 119.70 (CH), 35.90 (Cq), 30.45( $\text{CH}_2$ ), 30.35( $\text{CH}_3$ ). IR-ATR ( $\text{cm}^{-1}$ ): 3074 ( $\nu\text{CH}$ ), 2953 ( $\nu\text{CH}$ ), 2905 ( $\nu\text{CH}$ ),

2865 ( $\nu$ CH), 1615 ( $\nu$ C=C), 1539, 1485 ( $\nu$ C=C), 1462 ( $\delta$ CH<sub>2</sub>), 1414, 1394 ( $\delta$ CH<sub>3</sub>), 1365 ( $\nu$ CH<sub>3</sub>), 1283, 1265, 1251, 1202, 1154, 1123, 1076, 1030, 973, 926, 903, 869, 850, 826, 772, 733, 688, 672, 593, 564, 532, 481, 442, 416. UV-vis [CH<sub>2</sub>Cl<sub>2</sub>,  $\lambda_{\max}$  (nm) ( $\epsilon$  (M<sup>-1</sup>.cm<sup>-1</sup>))]: 635 (9,318 x 10<sup>3</sup>), 380 (7510), 300 (65200). MALDI-TOF-MS:  $m/z$  = 643.3 (M<sup>+</sup>) Anal. Calc. for C<sub>22</sub>H<sub>28</sub>N<sub>2</sub>PtS<sub>4</sub> (%): C 41.04, H 4.38, N 4.35. Found (%): C 41.05, H 4.53, N 4.27

## 7. Complex 2d

First, [PtCl<sub>2</sub>(bpy)] (0.048 g, 0.11 mmol) was reacted with 2.2 eq. of silver triflate (0.064 g, 0.25 mmol) in 5 mL of dry CH<sub>3</sub>CN under N<sub>2</sub> atmosphere for 4h. The suspension was filtered over celite to remove the formed silver chloride salt. After removal of the solvent, the residue was redissolved in 10 mL dry THF and 0.5 eq. of complex **6** were added (0.114 g, 0.055 mmol). The mixture was heated at reflux under N<sub>2</sub> for 3 days. After evaporation of the solvent, the product was purified by flash column chromatography on silica gel using a gradient of eluents for pure CH<sub>2</sub>Cl<sub>2</sub> to CH<sub>2</sub>Cl<sub>2</sub>+ 5 %v/v MeOH. After removal of the solvents, the product was isolated as a blue powder in 28 % yield (43 mg).

<sup>1</sup>H NMR (300 MHz, Chloroform-*d*)  $\delta$  9.30 (s, 2H, CH<sub>bpy</sub>), 7.99 – 7.84 (m, 4H, CH<sub>bpy</sub>/CH<sub>ph</sub>), 7.42 – 7.28 (m, 4H, CH<sub>bpy</sub>/CH<sub>ph</sub>), 6.83 – 6.65 (m, 4H, CH<sub>bpy</sub>/CH<sub>ph</sub>), 4.40 – 4.19 (m, 8H, OCH<sub>2</sub>), 2.11 – 1.89 (m, 8H, CH<sub>2</sub>), 1.73 – 1.12 (m, 72H, CH<sub>2</sub>), 1.05 – 0.73 (m, 12H, CH<sub>3</sub>). <sup>13</sup>C NMR (75 MHz, Chloroform-*d*)  $\delta$  31.99, 29.84, 29.81, 29.79, 29.76, 29.70, 29.45, 29.37, 26.53, 26.35, 22.73, 14.09, 0.99. Only the peaks of the carbon chains are visible at high concentration on the <sup>13</sup>C NMR spectra. IR-ATR (cm<sup>-1</sup>): 3081 ( $\nu$ CH), 2955 ( $\nu$ CH), 2917 ( $\nu$ CH), 2850 ( $\nu$ CH), 1605 ( $\nu$ C=C), 1540, 1497 ( $\nu$ C=C), 1469 ( $\delta$ CH<sub>2</sub>), 1449 ( $\delta$ CH<sub>2</sub>), 1431 ( $\delta$ CH<sub>2</sub>), 1414, 1382 ( $\delta$ CH<sub>3</sub>), 1313, 1257, 1237, 1182, 1131, 1068, 1031, 995, 958, 905, 842, 809, 787, 746, 716, 654, 629, 607, 413. UV-vis [CH<sub>2</sub>Cl<sub>2</sub>,  $\lambda_{\max}$  (nm) ( $\epsilon$  (M<sup>-1</sup>.cm<sup>-1</sup>))]: 660 (11020), 348 (34500), 304 (91900), 270 (117300), 254 (138800). MALDI-TOF-MS:  $m/z$  = 1329.4 (M<sup>+</sup>). Anal. Calc. for

C<sub>72</sub>H<sub>114</sub>N<sub>2</sub>O<sub>4</sub>PtS<sub>2</sub>, 0.2 CH<sub>2</sub>Cl<sub>2</sub> (%): C 64.34, H 8.55, N 2.08 S 4.76. Found (%): C 64.45, H 8.76, N 1.83 S 4.81.

## 8. Complex 1b

Complex **4b** (0.09 g, 0.07 mmol) were dissolved in 10 mL acetone with 5 mL THF and one equivalent of 2,2-Dibutyl-5,6-dihydro-1,3,2-dithiastannolo[4,5-b][1,4]dithiin (0.032 g, 0.07 mmol) was added. The reaction mixture was stirred at room temperature under N<sub>2</sub> atmosphere. After 3 days, the green precipitate, which has formed, was filtered, washed with acetone and dried. The compound was next dissolved in CH<sub>2</sub>Cl<sub>2</sub>, filtered over celite to remove the insoluble and recrystallized in CH<sub>3</sub>CN. The compound was isolated as a green powder in 63 % yield (62 mg).

<sup>1</sup>H NMR (300 MHz, Chloroform-*d*) δ 9.75 (d, *J* = 6.0 Hz, 2H, CH<sub>bpy</sub>), 8.57 (d, *J* = 1.8 Hz, 2H, CH<sub>bpy</sub>), 8.04 (dd, *J* = 6.0, 1.7 Hz, 2H, CH<sub>bpy</sub>), 7.73 – 7.56 (m, 8H, CH<sub>biph</sub>), 7.54 – 7.45 (m, 4H, CH<sub>biph</sub>), 7.01 – 6.92 (m, 4H, CH<sub>biph</sub>), 4.46 (t, *J* = 6.8 Hz, 4H, OCH<sub>2</sub>), 3.99 (t, *J* = 6.5 Hz, 4H, OCH<sub>2</sub>), 2.61 (s, 4H, CH<sub>2dithio</sub>), 1.95 – 1.74 (m, 8H, CH<sub>2</sub>), 1.59 – 1.16 (m, 24H, CH<sub>2</sub>). <sup>13</sup>C NMR (75 MHz, Chloroform-*d*) δ 163.13 (Cq), 159.89 (Cq), 157.49 (Cq), 150.30 (CH), 145.31 (Cq), 140.50 (Cq), 132.68 (CH), 131.33 (Cq), 128.42 (CH), 127.15 (CH), 126.92 (CH), 123.22 (CH), 119.20 (Cq), 115.20 (CH), 110.15 (Cq), 68.28 (OCH<sub>2</sub>), 67.48 (OCH<sub>2</sub>), 41.12 (Cq), 32.91 (CH<sub>2</sub>), 29.82 (CH<sub>2</sub>), 29.57 (CH<sub>2</sub>), 29.53 (CH<sub>2</sub>), 29.47 (CH<sub>2</sub>), 29.35 (CH<sub>2</sub>), 29.32 (CH<sub>2</sub>), 28.64 (CH<sub>2</sub>), 26.16 (CH<sub>2</sub>), 25.99 (CH<sub>2</sub>), 22.81 (CH<sub>2</sub>). IR-ATR (cm<sup>-1</sup>): 3070 (νCH), 2923 (νCH), 2853 (νCH), 2224 (νCN), 1723 (νC=O), 1602 (νC=C), 1580, 1494 (νC=C), 1469 (δCH<sub>2</sub>), 1433 (δCH<sub>2</sub>), 1409, 1321 (δCH<sub>3</sub>), 1292, 1249, 1180, 1131, 1032, 999, 958, 852, 821, 758, 723, 703, 661, 562, 531, 414. UV-vis [CH<sub>2</sub>Cl<sub>2</sub>, λ<sub>max</sub> (nm) (ε (M<sup>-1</sup>.cm<sup>-1</sup>))]: 808 (7540), 528 (2425), 440 (2690), 377 (5320), 300 (61230). MALDI-TOF-MS: *m/z* = 1285.4 (M<sup>+</sup>). Anal. Calc. for C<sub>62</sub>H<sub>66</sub>N<sub>4</sub>O<sub>6</sub>PtS<sub>4</sub>, 0.5 CH<sub>2</sub>Cl<sub>2</sub> (%): C 56.48, H 5.08, N 4.22, S 9.65. Found (%): C 56.11, H 5.02, N 4.17 S 9.48.

## 9. Complex 2a

Complex **4a** (0.055 g, 0.03 mmol) was reacted with 2.2 eq. of silver triflate (0.018 g, 0.07 mmol) in 10 mL of dry THF under N<sub>2</sub> atmosphere for 24h. The suspension was filtered over celite to remove the formed silver chloride salt. 0.5 eq. of complex **6** (0.03 g, 0.015 mmol) were then added to the filtrate and the mixture was heated at reflux under N<sub>2</sub> for 60 h. After evaporation of the solvent, the product was purified by flash column chromatography on silica gel using CH<sub>2</sub>Cl<sub>2</sub>+ 1 % v/v MeOH as eluent. After drying, the product was isolated as a green powder in 43 % yield (36 mg).

Despite several attempts (CDCl<sub>3</sub>, d<sub>6</sub>-DMSO, CD<sub>2</sub>Cl<sub>2</sub>), no clear <sup>1</sup>H and <sup>13</sup>C NMR spectra has been obtained for this compound. IR-ATR (cm<sup>-1</sup>): 3072 (νCH), 2956 (νCH), 2921 (νCH), 2852 (νCH), 1725 (νC=O), 1667 (νC=O), 1603 (νC=C), 1546 (δNH), 1505 (νC=C), 1466 (δCH<sub>2</sub>), 1429, 1379 (δCH<sub>3</sub>), 1262, 1115, 1074, 1019, 802, 731. UV-vis [CH<sub>2</sub>Cl<sub>2</sub>, λ<sub>max</sub> (nm) (ε (M<sup>-1</sup>.cm<sup>-1</sup>))]: 626 (6910), 430 (16830), 306 (72740). MALDI-TOF-MS: *m/z* = 2674.2 (M<sup>+</sup>). Anal. Calc. for C<sub>158</sub>H<sub>268</sub>N<sub>4</sub>O<sub>12</sub>PtS<sub>2</sub>, 2CH<sub>2</sub>Cl<sub>2</sub> (%): C 67.55, H 9.64, N 1.97, S 2.25. Found (%): C 67.62, H 9.22, N 1.76, S 2.39.

## 10. Complex 2b

25 mg of complex **4b** (0.02 mmol) were reacted with 2.2 eq. of silver triflate in 5 mL of CH<sub>3</sub>CN under N<sub>2</sub> atmosphere for 17 h. The solution was filtered over celite and 0.5 eq. of complex **6** (0.021 g, 0.01 mmol) were then added to the filtrate and the mixture was heated at reflux under N<sub>2</sub> for 48 h. After evaporation of the solvent, the product was purified by column chromatography on silica gel using a gradient of eluent from CH<sub>2</sub>Cl<sub>2</sub>+ 1% v/v THF to CH<sub>2</sub>Cl<sub>2</sub>+ 5% v/v THF. The product was isolated as a blue compound in 42 % yield (18.5 mg).

Despite several attempts (CDCl<sub>3</sub>, d<sub>6</sub>-DMSO, CD<sub>2</sub>Cl<sub>2</sub>), no clear <sup>1</sup>H and <sup>13</sup>C NMR spectra has been obtained for this compound. IR-ATR (cm<sup>-1</sup>): 3076 (νCH), 2920 (νCH), 2851 (νCH), 2225 (νCN), 1724 (νC=O), 1603 (νC=C), 1581, 1509, 1495 (νC=C), 1467 (δCH<sub>2</sub>), 1429 (δCH<sub>2</sub>), 1413, 1381 (δCH<sub>3</sub>), 1261, 1246, 1180, 1138, 1117, 1063, 1030, 927, 896, 850, 804, 759, 730, 706, 661, 636, 606, 563, 531. UV-vis [CH<sub>2</sub>Cl<sub>2</sub>, λ<sub>max</sub> (nm) (ε (M<sup>-1</sup>.cm<sup>-1</sup>))]: 816 (12880), 298 (216050). MALDI-TOF-MS: *m/z* = 2085.19 (M<sup>+</sup>). Anal. Calc. for C<sub>120</sub>H<sub>168</sub>N<sub>4</sub>O<sub>10</sub>PtS<sub>2</sub>, 2/3 CH<sub>2</sub>Cl<sub>2</sub> (%): C 67.65, H 7.97, N 2.62, S 2.99. Found (%): C 67.70, H 8.60, N 1.90 S 2.60.

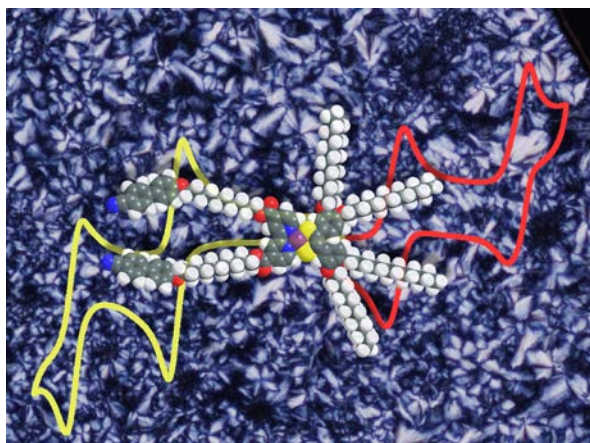
**Keywords:** Platinum diimine dithiolene • Coordination chemistry • Liquid crystal  
• Ambipolar • Charge transfer

#### **Acknowledgements.**

The CNRS, Rennes Metropole and the University of Rennes 1 are gratefully acknowledged for financial support. This work was granted access to the high performance computing resources of CINES (Montpellier, France) under allocation 2018-A0040805032 awarded by GENCI. Antoine Vacher is gratefully acknowledged for his help in the solid-state absorption measurements.

**Supporting Information description.** UV-vis-NIR absorption spectra, emission spectra and cyclic voltammograms of all the compounds as well as additional DSC, POM and X-rays analyses. CCDC 1867102 contains the supplementary crystallographic data for complex **1c**. These data can be obtained free of charge from The Cambridge Crystallographic Data Centre via [www.ccdc.cam.ac.uk/data\\_request/cif](http://www.ccdc.cam.ac.uk/data_request/cif).

**TOC.**



Highly functional mesogens constructed around ambipolar platinum diimine-dithiolene cores have been isolated through an original ligand metathesis approach.

## References.

- [1] a) T. Wöhrle, I. Wurzbach, J. Kirres, A. Kostidou, N. Kapernaum, J. Litterscheidt, J.C. Haenle, P. Staffeld, A. Baro, F. Giesselmann, S. Laschat, *Chem Rev.* **2016**, *116*, 1139-1241; b) S. Kumar, CRC Press, Boca Raton, USA, **2011**; c) S. Setia, S. Sidiq, J. De, I. Pani, S.K. Pal, *Liq Cryst.* **2016**, *43*, 2009-2050; d) R.K. Gupta, V. Manjuladevi, C. Karthik, K. Choudhary, *Liq Cryst.* **2016**, *43*, 2079-2091; e) S.M. Said, M.S. Mahmood, M.N. Daud, M.F. Mohd Sabri, N.A. Sairi, *Liq Cryst.* **2016**, *43*, 2092-2113.
- [2] a) H. Iino, J. Hanna, *Opto-Electron. Rev.* **2005**, *13*, 295-302; b) S. Sergeev, W. Pisula, Y. H. Geerts, *Chem. Soc. Rev.* **2007**, *36*, 1902-1929; c) M. Funahashi, *Polym. J.* **2009**, *41*, 459-469.
- [3] A) H. Iino, J. Hanna, *opto-electronics review* **2005**, *13*, 295-302; b) H. Monobe, Y. Shimizu, S. Okamoto, H. Enomoto, *Mol. Cryst. Liq. Cryst.* **2007**, *476*, 31/[277]-41/[287].
- [4] T. Yasuda, T. Shimizu, F. Liu, G. Ungar, T. Kato, *J. Am. Chem. Soc.* **2011**, *133*, 13437-13444.
- [5] (a) G. Bottari, G. de la Torres, D.M. Guldi, T. Torres, *Chem. Rev.* **2010**, *110*, 6768-6816; (b) A. de la Escosura, M.V. Martinez-Diaz, J. Barbera, T. Torres, *J. Org. Chem.* **2008**, *73*, 1475-1480; (c) Y.H. Geerts, O. Debever, C. Amato, S. Sergeev, *Beilstein J. Org. Chem.* **2009**, *5*, DOI:10.3762/bjoc.5.49; (d) M. Ince, M.V. Martinez-Diaz, J. Barbera, T. Torres, *J. Mater. Chem.* **2011**, *21*, 1531-1536.
- [6] P. Samorì, A. Fechtenkötter, E. Reuther, M. Watson, N. Severin, K. Müllen, J. Rabe, *Adv. Mater.* **2006**, *18*, 1317-1321.
- [7] X. Liu, T. Usui, J. Hanna, *Chem. Mater.* **2014**, *26*, 5437-5440.
- [8] T. Kushida, A. Shuto, M. Yoshio, T. Kato, S. Yamaguchi, *Angew. Chem. Int. Ed.* **2015**, *54*, 6922-6925.
- [9] Seema Barard, Theo Kreouzis, Andrew N Cammidge, Michael J Cook, Asim K Ray, *Semicond. Sci. Technol.* **2018**, *33*, 095010.
- [10] H. Hayashi, W. Nishihara, T. Umeyama, Y. Matano, S. Seki, Y. Shimizu, H. Imahori, *J. Am. Chem. Soc.* **2011**, *133*, 10736-10739.
- [11] H. Geng, K. Luo, G. Zou, L. Zhao, H. Wang, Q. Li, H. Ni, *Dyes and Pigments* **2018**, *149*, 82-91.
- [12] a) T. Kusamoto, S. Kume, H. Nishihara, *J. Am. Chem. Soc.* **2008**, *130*, 13844-13845; b) W. Liu, R. Wang, X.-H. Zhou, J.-L. Zuo, X.-Z. You, *Organometallics* **2008**, *27*, 126-134.
- [13] a) W. Paw, S.D. Cummings, M. Adnan Mansour, W.B. Connick, D.K. Geiger, R. Eisenberg, *Coord. Chem. Rev.* **1998**, *171*, 125-150; b) S.D. Cummings, R. Eisenberg, *Inorg. Chem.* **1995**, *34*, 2007-2014; c) J.A. Zuleta, C.A. Chesta, R. Eisenberg, *J. Am. Chem. Soc.* **1989**, *111*, 8916-8917; d) J.A. Zuleta, J.M. Bevilacqua, D.M. Proserpio, P.D. Harvey, R. Eisenberg, *Inorg. Chem.* **1992**, *31*, 12, 2396-2404.
- [14] a) J. Zhang, P. Du, J. Schneider, P. Jarosz, R. Eisenberg, *J. Am. Chem. Soc.* **2007**, *129*, 7726-7727; b) G. Li, M. F. Mark, H. Lv, D.W. McCamant, R. Eisenberg, *J. Am. Chem. Soc.* **2018**, *140*, 2575-2586.

- [15] a) B.W. Smucker, J.M. Hudson, M.A. Omary, K.R. Dunbar, *Inorg. Chem.* **2003**, *42*, 4714-4723; b) K. Diwan, R. Chauhan, S.K. Singh, B. Singh, M.G. B. Drew, L. Bahadura, N. Singh, *New J. Chem.* **2014**, *38*, 97-108.
- [16] a) Y. Ji, R. Zhang, X.-B. Du, J.-L. Zuo, X.-Z. You, *Dalton Trans.* **2008**, 2578-2582; b) Y. Ji, R. Zhang, Y.-J. Li, Y.-Z. Li, J.-L. Zuo, X.-Z. You, *Inorg. Chem.* **2007**, *46*, 866-873.
- [17] H.-C. Chang, K. Komasa, K. Kishida, T. Shiozaki, T. Ohmori, T. Matsumoto, A. Kobayashi, M. Kato, S. Kitagawa, *Inorg. Chem.* **2011**, *50*, 4279-4288.
- [18] C.E. Whittle, J.A. Weinstein, M.W. George, K.S. Schanze, *Inorg. Chem.* **2001**, *40*, 4053-4062.
- [19] B. Huitorel, Q. Benito, A. Fargues, A. Garcia, T. Gacoin, J.-P. boilot, S. Perruchas, F. Camerel, *Chem. Mater.* **2016**, *28*, 8190-8200.
- [20] a) C.-W. Chan, L.-K. Cheng, C.-M. Che, *Coord. Chem. Rev.* **1994**, *132*, 87-97; b) T.J. Wadas, R.J. Lachicotte, R. Eisenberg, *Inorg. Chem.* **2003**, *42*, 3772-3778; c) V.M. Miskowski, V.H. Houlding, C.-M. Che, Y. Wang, *Inorg. Chem.* **1993**, *32*, 2518-2524.
- [21] a) S.D. Cummings, R. Eisenberg, *J. Am. Chem. Soc.* **1996**, *118*, 1949-1960; b) W.B. Connick, H.B. Gray, *J. Am. Chem. Soc.* **1997**, *119*, 11620-11627.
- [22] K. Nakamaru, *Bull. Chem. Soc. Jpn* **1982**, *55*, 1639-1640.
- [23] S. Campidelli, J. Lenoble, J. Barbera, F. Paolucci, M. Marcaccio, D. Paolucci, R. Deschenaux, *Macromolecules* **2005**, *38*, 7915-7925;
- [24] A. Gennaro, A.A. Isse, J.-M. Savéant, M.G. Severin, E. Vianello, *J. Am. Chem. Soc.* **1996**, *118*, 7190-7196
- [25] E.J.L. McInnes, R.D. Farley, C.C. Rowlands, A.J. Welch, L. Rovatti, L.J. Yellowlees, *J. Chem. Soc., Dalton Trans.*, **1999**, 4203-4208;
- [26] Y. Misaki, Y. Tani, K. Takahashi, K. Tanaka, *Molecular Crystals and Liquid Crystals* (2002), *379*, 71-76.
- [27] F. Camerel, F. Kinloch, O. Jeannin, M. Robin, S. K. Nayak, E. Jacques, K. A. Brylev, N. G. Naumov, Y. Molard, *Dalton Trans.*, **2018**, *47*, 10884-10896.
- [28] S. Debnath, H. F. Srour, B. Donnio, Marc Fourmigué, F. Camerel, *RSC Adv.* **2012**, *2*, 4453-4462.
- [29] F. Camerel, R. Ziessel, B. Donnio, C. Bourgoigne, D. Guillon, M. Schmutz, C. Iacovita, J.-P. Bucher, *Angew. Chem. Int. Ed.*, **2007**, *46*, 2659-2662
- [30] A. Altomare, G. Cascarano, C. Giacovazzo, A. Guagliardi, M. C. Burla, G. Polidori, M. Camalli, *J. Appl. Cryst.* **1994**, *27*, 435.
- [31] G. M. Sheldrick, *Acta Cryst. C* **2015**, *71*, 3-8.
- [32] L.J.J. Farrugia, *Appl. Cryst.* **2012**, *45*, 849-854.
- [33] a) P. Hohenberg and W. Kohn, *Phys. Rev.* **1964**, *136*, B864-B871; b) R.G. Parr, W. Yang, *Density-Functional Theory of Atoms and Molecules*; Oxford University Press: Oxford, U.K., **1989**.
- [34] a) A. D. Becke, *Phys. Rev. A* **1988**, *38*, 3098-3100; b) A. D. Becke, *J. Chem. Phys.* **1993**, *98*, 1372-1377; c) A. D. Becke, *J. Chem. Phys.* **1993**, *98*, 5648-5652.
- [35] C. Lee, W. Yang, R. G. Parr, *Phys. Rev. B* **1988**, *37*, 785-789.
- [36] M. J. Frisch, G. W. Trucks, H. B. Schlegel, G. E. Scuseria, M. A. Robb, J. R. Cheeseman, G. Scalmani, V. Barone, B. Mennucci, G. A. Petersson, H. Nakatsuji, M. Caricato, X. Li, H. P. Hratchian, A. F. Izmaylov, J. Bloino, G. Zheng, J. L. Sonnenberg, M. Hada, M. Ehara, K. Toyota, R. Fukuda, J. Hasegawa, M. Ishida, T. Nakajima, Y. Honda, O. Kitao, H. Nakai, T. Vreven, J. A. J. Montgomery, J. E. Peralta, F. Ogliaro, M. Bearpark, J. J. Heyd, E. Brothers, K. N. Kudin, V. N. Staroverov, T. Keith, R. Kobayashi, J. Normand, K. Raghavachari, A. Rendell, J. C. Burant, S. S. Iyengar, J. Tomasi, M. Cossi, N. Rega, J. M. Millam, M. Klene, J. E. Knox, J. B. Cross, V. Bakken, C. Adamo, J. Jaramillo, R. Gomperts, R. E. Stratmann, O. Yazyev, A. J. Austin, R. Cammi, C. Pomelli, J. W. Ochterski, R. L. Martin, K. Morokuma, V. G. Zakrzewski, G. A. Voth, P. Salvador, J. J. Dannenberg, S. Dapprich, A. D. Daniels, O. Farkas, J. B. Foresman, J. V. Ortiz, J. Cioslowski, D. J. Fox, Gaussian 09, Revision B.01, Gaussian, Inc., Wallingford CT, **2010**.
- [37] J. Bai, H. Wei, B. Li, L. Song, L. Fang, Z. Lv, W. Zhou, E. Wang, *Chem. Asian J.* **2008**, *3*, 1935-1941.
- [38] C.V. Yelamaggad, A.S. Achalkumar, D.S.S. Rao, S.K. Prasad, *J. Org. Chem.* **2007**, *72*, 8308-8318.
- [39] K. Ohta, Y. Inagaki-Oka, H. Hasebe and I. Yamamoto, *Polyhedron* **2000**, *19*, 267-274.
- [40] C.V. Yelamaggad, V.P. Tamilenthir, *Tetrahedron* **2009**, *65*, 6403-6409.
- [41] a) K.D. Hodges, J.V. Rund, *Inorg. Chem.* **1975**, *14*, 525-528; b) A. Vacher, F. Barrière, F. Camerel, J.-F. Bergamini, T. Roisnel, D. Lorcy, *Dalton Trans.* **2013**, *42*, 383-394.
- [42] S.-K. Lee, K.-S. Shin, D.-Y. Noh, O. Jeannin, F. Barriere, J.-F. Bergamini, M. Fourmigue, *Chem. Asian J.* **2010**, *5*, 169-176.
- [43] J.H. Price, J.P. Birk, B.B. Wayland, *Inorg. Chem.* **1978**, *17*, 2245-2250.